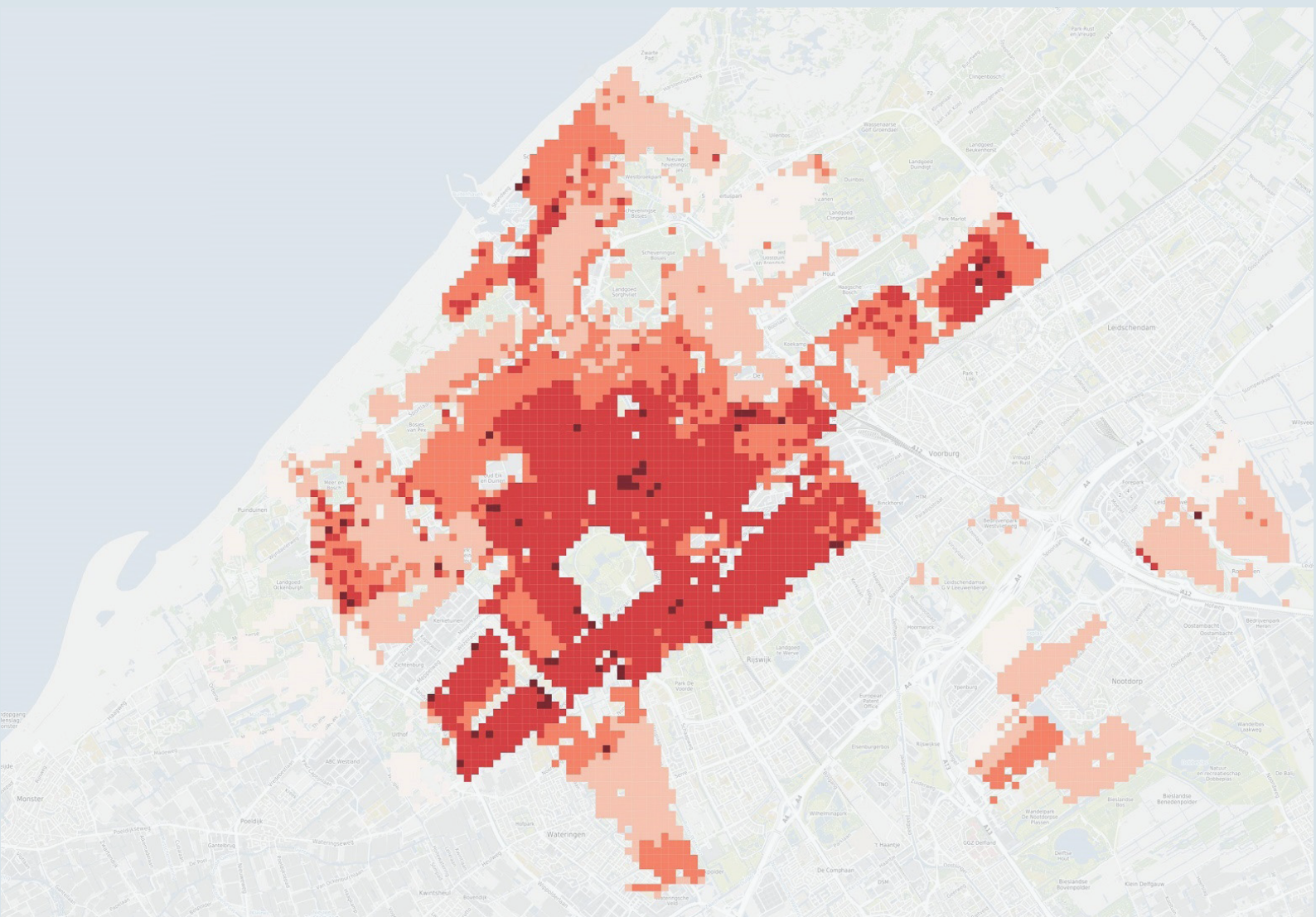


Modelling the risks of urban heat islands for the ageing society

Case study: The Hague

MSc thesis Geomatics in the built environment
Noortje Vaissier 4206479



MODELLING THE RISKS OF URBAN HEAT ISLANDS FOR THE
AGEING SOCIETY. CASE STUDY: THE HAGUE

A thesis submitted to the Delft University of Technology in partial fulfillment
of the requirements for the degree of

Master of Science in Geomatics for the Built Environment

by

Noortje Vaissier

October 2019

A thesis submitted to the Delft University of Technology in partial fulfilment of the requirements for the degree of

Master of Science in Geomatics

by

Noortje Vaissier

October 2019

Supervising Professor: Dr.ir. F.D. van der Hoeven
Supervisor: Dipl.ing. A. Wandl
Co-reader: Dr.ir. Bastiaan van Loenen

Noortje Vaissier: *Modelling the risks of urban heat islands for the ageing society of the Hague* (2019)

© This work is licensed under a Creative Commons Attribution 4.0 International License. To view a copy of this license, visit <http://creativecommons.org/licenses/by/4.0/>.

ISBN 999-99-9999-999-9

The work in this thesis was made in the:

Department of Urbanism
Faculty of Architecture & the Built Environment
Delft University of Technology

Supervisors: Alexander Wandl
Frank van der Hoeven
Co-reader: Bastiaan van Loenen

ABSTRACT

Heat waves are a leading cause of weather related fatalities world-wide. Due to increasing urbanisation, climate change and an ageing population, health risks for urban populations will continue to increase in the coming years. The effect of urban heat islands on the health of vulnerable groups where especially the elderly population is hit the hardest, is widely recognized in literature.

In past studies the effect of heat has been modelled for the entire population of a city or state where outside temperature measures or land surface temperature is the hazard. Research on specific vulnerable groups such as the elderly is relatively sparse to this date. In this study various datasets have been combined with the aim of providing a method for the development of a heat-related elderly risk index (HERI) for the elderly population of The Hague. The final composite risk indexes have been constructed for three moments in the day on the 27th of July which was the hottest day of the heat wave of 2018.

The structure of the index is based on Crichton's Triangle of Risk, which states that risk is a function of hazard, exposure, and vulnerability. By selecting the following indicators to represent the spatial layers: physiological equivalent temperature, indoor temperature, facade orientation, being 75 years or older, loneliness among people over the age of 75, and population density. The indicators are assigned a weight through the Analytical Hierarchy Process (AHP), after which the indicators can be combined into a HERI maps for the three timestamps. Different configurations of indicators have been used for creating the HERI maps, yielding different weights for each set. This resulted in two types of HERI maps: HERI-2 and HERI-3. HERI-2 consists of physiological equivalent temperature, being 75 years or older, loneliness among people over the age of 75, and population density. HERI-3 is composed of the same indicators as HERI-2 but instead of physiological equivalent temperature, indoor temperature is used as the hazard.

The HERI maps for the three timestamps have been validated by performing a Pearson Correlation between the HERI maps and the mortality numbers among the elderly in the days after the heat wave. The indicators and mortality are non correlated except for the indicator 'being 75 years or older'. However when the indicators are combined into the HERI index maps a weak positive correlation with mortality can be seen. The results indicate that it is necessary that the indicators have to be re-evaluated and several weighting methods have to be considered in order to improve the HERI.

ACKNOWLEDGEMENTS

I would like to thank several people for giving me support during my studies. Firstly I would like to thank my supervisors Alexander Wandl and Frank van der Hoeven for brainstorming with me during my thesis, their supervision and guidance has been very beneficial.

Furthermore I want to thank Daniela Maiullari for her very helpful insights and thoughts on how to proceed at the beginning of my thesis and with providing me with the right software and computers to execute the heavy simulations. Also I would like to say thanks to Marjolein Pijpers-van Esch for connecting me with experts in the field and the license I needed for using ENVI-met. I want to thank Arie Romein for helping me with statistics at the end of my thesis.

Last but not least I would like to thank my friends and family with providing with their listening ear and support. A special thanks to my friend Marco to take time out of his day to read my thesis, when he could be exploring Delft.

CONTENTS

1	INTRODUCTION	1
1.1	Problem statement	1
1.1.1	Scope and research questions	2
1.2	Reading guide	3
2	THEORETICAL BACKGROUND	5
2.1	The heatwave of July 2018	5
2.2	Urban heat islands	6
2.3	Outdoor thermal comfort	8
2.4	Weighting and aggregation of spatial layers	9
2.4.1	Equal weights method	9
2.4.2	Ordered weighted averaging method (OWA)	10
2.4.3	Weighted linear combination method (WLC)	10
2.4.4	Analytical Hierarchy Process method (AHP)	10
3	RELATED WORK	13
3.1	Report on The Hague: Haagse Hitte	13
3.2	Heat vulnerability indexes	13
3.2.1	Heat Vulnerability Index (HVI) for Birmingham	14
3.3	Mapping of heat-related risks for the elderly in Italy	15
3.4	Social determinants of heat vulnerability	15
3.4.1	Loneliness amongst the elderly	16
3.5	Spatial determinant of heat vulnerability	16
3.5.1	Indoor temperature and the orientation of the facade	16
3.6	Validation of heat risk maps	17
4	METHODOLOGY	19
4.1	Literature and related work review	19
4.2	Sensor data retrieval, storage, cleaning and analyses	19
4.3	Collection, aggregation and analyses of added spatial data	19
4.4	Defining the spatial layers	20
4.4.1	Hazard layer	20
4.4.2	Exposure layer	20
4.4.3	Vulnerability layers	20
4.5	Weighting procedure	21
4.6	Mapping HERI	21
4.7	Validation	22
4.8	Tools and datasets	23
4.8.1	Tools	23
4.8.2	Datasets	25
5	SENSOR DATA	27
5.1	Tropical days	27
5.2	Using the temperatures to validate the ENVI-met models	28
5.3	Quby sensors	28
6	PREPARATION SPATIAL LAYERS FOR THE INDEX	29
6.1	Hazard layer: PET	29
6.1.1	Selection of the locations	30
6.1.2	Simulation set-up	30
6.1.3	Biomet	31
6.1.4	PET results	32
6.1.5	Mean radiant Temperature	32
6.2	Hazard layer: Indoor temperature	34
6.3	Exposure layer	34
6.4	Vulnerability layer	35

7	DEVELOPING THE HERI	37
7.1	AHP Results	37
7.1.1	AHP result Set-1	38
7.1.2	AHP result Set-2 and Set-3	39
7.2	Composing HERI maps	40
7.2.1	HERI-1	40
7.2.2	HERI-2	42
7.2.3	HERI-3	45
7.3	Validation of the HERI	47
7.3.1	Bivariate Pearson Correlation	47
7.3.2	Conclusion validation	49
8	CONCLUSIONS	51
8.1	Research questions	51
8.2	Contribution and reflection	52
8.3	Future work and recommendations	54
9	DISCUSSION	55
A	QUESTIONNAIRE	57
B	SCRIPT FOR FILLING THE DATABASE	59
C	SPATIAL LAYERS	61
D	INDEXES	67

LIST OF FIGURES

Figure 1.1	The municipality of The Hague [Ntarladima, 2016]	2
Figure 2.1	Number of people deceased per week in 2018 (in green) and of 2006(in green), and the average number of deceased people of 2015, 2016, 2017 together (in dark blue) [Centraal Bureau voor de Statistiek, 2018].	5
Figure 2.2	In light blue the deads in week 29, 30 and 31 of 2018. In dark blue deads in week 29, 30 and 31 of the years 2015, 2016 and 2017. And in green the deads in 2006 of week 27, 29 and 30 [Centraal Bureau voor de Statistiek, 2018].	6
Figure 2.3	PBL, UBL and UCL [Duffy et al., 2010]	7
Figure 2.4	Variations of surface and atmospheric temperatures (EPA,2017)	7
Figure 2.5	Hierarchical tree structure of AHP [Siddayao et al., 2014]	11
Figure 3.1	Crichtons triangle of risk [Tomlinson et al., 2011]	14
Figure 3.2	Workflow of the GIS spatial risk assessment methodology used to assess Birmingham[Tomlinson et al., 2011]	14
Figure 3.3	Morabito workfow [Morabito et al., 2015]	15
Figure 3.4	Subdivision of street canyon according to climatic design needs[Ali-Toudert, 2007]	17
Figure 4.1	Workflow, based on Morabito et al. [2015].	21
Figure 4.2	Methodology research	22
Figure 4.3	Database containing the Netatmo measurements in PostgreSQL	23
Figure 4.4	Simple layout of ENVI-met’s fluid dynamics model [Rosheidat et al., 2008].	24
Figure 4.5	The human parameters that can be adjusted in the Biomet tool for calculating Physiological Equivalent Temperature (PET) values.	24
Figure 4.6	Data flow within the ENVI-met environment [Maleki et al., 2014].	24
Figure 4.7	Interface of the Haagse Bomen App	25
Figure 4.8	Netatmo sensors	26
Figure 5.1	Diagram depicting how many times the sensors have measured temperatures above 30 °C for each day over the period 05/02/2018 till 09/30/2018.	27
Figure 6.1	Map containing the nine locations (in blue dots) throughout The Hague where the PET values have been calculated.	29
Figure 6.2	Weesperstraat	31
Figure 6.3	For all the timestamps the average, median and modus of the PET calculated for a man aged 75.	32
Figure 6.4	Tmrt at 14.00 o’clock in the Weesperstraat.	33
Figure 6.5	PET at 14.00 o’clock in the Weesperstraat.	33
Figure 6.6	Orientations.	34
Figure 7.1	The consolidation matrix of Set-1.	38
Figure 7.2	Consolidation matrices of Set-2 and Set-3.	39
Figure 7.3	Spatial layers from left to right: Loneliness amongst elderly, population density, and people above the age of 75. These spatial layers are the same in the creation of Heat-related Elderly Risk Index (HERI) maps for every timestamp.	40
Figure 7.4	HERI-1 at 14.00 o’clock in the afternoon.	41
Figure 7.5	From left to right: PET temperatures for 04.00 o’clock, 14.00 o’clock, and 24.00 o’clock.	42

Figure 7.6	HERI-2 maps for the the three timestamps.	44
Figure 7.7	From left to right: indoor temperatures for 04.00 o'clock, 14.00 o'clock, and 24.00 o'clock.	45
Figure 7.8	HERI-3 maps for the the three timestamps.	46
Figure 7.9	Number of deceased people of 75 or over between July 27th to July 31st 2018, together with the HERI-3 at 24.00 o'clock. . .	48
Figure 7.10	The correlation values of HERI-2 indicators with mortality amongst the elderly and their significance.	48
Figure 7.11	The correlation values of HERI-2 maps with mortality amongst the elderly and their significance.	48
Figure 7.12	Correlation of indicators with mortality used to create HERI-3.	49
Figure 7.13	The correlation values of HERI-2 maps with mortality amongst the elderly and their significance.	49
Figure A.1	57
Figure A.2	58
Figure B.1	59
Figure B.2	60
Figure C.1	Population density in the city of The Hague.	61
Figure C.2	Population above the age of 75 in the city of The Hague. . . .	62
Figure C.3	Streets displaying structure of The Hague.	62
Figure C.4	Orientation of facades divided into tile structure.	63
Figure C.5	The number of people using a thermometer to measure the temperature in their homes aggregated at neighbourhood level.	63
Figure C.6	Indoor temperature measured inside homes at the 27th of July at 14.00 o'clock, aggregated at neighbourhood level. . . .	64
Figure C.7	Percentage of lonely elderly (75+) for every neighbourhood. . .	64
Figure C.8	Percentage of lonely elderly (75+) tiles.	65
Figure D.1	HERI-2 at 04.00 o'clock in the morning at the 27th of July. . . .	67
Figure D.2	HERI-2 at 14.00 o'clock in the afternoon at the 27th of July. . .	68
Figure D.3	HERI-2 at 24.00 o'clock at night at the 27th of July.	68
Figure D.4	HERI-3 at 04.00 o'clock in the morning at the 27th of July. . . .	69
Figure D.5	HERI-3 at 14.00 o'clock in the afternoon at the 27th of July. . .	69
Figure D.6	HERI-3 at 24.00 o'clock at night at the 27th of July.	70

LIST OF TABLES

Table 2.1	PET table categorized regarding thermal stress [Matzarakis et al., 2014]	9
Table 2.2	Fundamental scale of absolute numbers [Saaty, 2008]	11
Table 2.3	Random Inconsistency index [Saaty, 2008]	11
Table 3.1	Triple index [Arup, 2014]	16
Table 6.1	The selected locations in The Hague together with the amount of people and elderly living in the selected 100m tile.	30
Table 6.2	Parameters used for every simulation in ENVI-met.	31
Table 6.3	Parameters used for calculating PET values for woman and men.	31
Table 7.1	Explanation of the indicators of heat vulnerability for the elderly population in the questionnaire.	37
Table 7.2	The three sets of indicators to make HERI-1, HERI-2, HERI-3 and HERI-4.	38
Table 7.3	Set-1 indicator weights.	38
Table 7.4	Set-2 indicator weights.	39
Table 7.5	Set-3 indicator weights.	39
Table 7.6	Weights tables and their absolute errors.	39

ACRONYMS

GIS	Geographical Information System	9
UHI	Urban Heat Island	1
HERI	Heat-related Elderly Risk Index	xiii
HVI	Heat Vulnerability Index	xi
KNMI	Koninklijk Nederlands Meteorologisch Instituut	1
AHP	Analytical Hierarchie Process	9
AHN	Actueel Hoogtebestand Nederland	26
PET	Physiological Equivalent Temperature	xiii
MCDM	Multi-Criteria Decision Making	9
OWA	Ordered Weighted Averaging	9
WLC	Weighted Linear Combination	10
PCM	Pairwise Comparison Matrice	10
RIVM	Rijks Instituut voor Volksgezondheid en Milieu	26
AHN	Algemeen Hoogtebestand Nederland	26
CR	Consistency Ratio	38
QGIS	Quantum Geographical Information System	23
CBS	Centraal Bureau Statistiek	5
OSM	Open Street Map	26
MEMI	Munich Energy-balance Model for individuals	8
SPSS	Statistical Package for the Social Sciences	25

1

INTRODUCTION

Since 2007, more than half of the world's population has been inhabiting cities [Gago et al., 2013]. A rapid increase of urban populations can be observed as more and more people migrate from rural areas to cities [Madlener and Sunak, 2011]. According to Mirzaei and Haghighat [2010] worldwide, the number of people inhabiting cities will increase to 60 percent (5.0 billion) by the year 2030. With the increase of urbanisation, climate change, and an ageing population, health risks for urban populations will continue to increase in the future [Lu, 2016]. Coincidental with climate change several types of extreme weather events are foreseen to increase in frequency, intensity and duration in the upcoming years. These include severe heat waves, or heavy rainfall with periods of drought afterwards [Gerald and Tebaldi, 2004].

A recent example of a high impact heat wave occurred during the summer of 2003 in Europe. The average temperature was 3.5 degrees above normal making it Europe's hottest summer in over 500 years [Lu, 2016]. Especially the city of Paris was hit severely by the heat wave, resulting in nearly 15.000 extra deaths in France, with the elderly population being affected in particular [Vandentorren et al., 2006]. No universal definition of a heat wave in literature exists. According to the Koninklijk Nederlands Meteorologisch Instituut (KNMI) the definition of a heat wave in the Netherlands is a sequence of five summer days or more measured in the Bilt (maximum temperature is 25,0°C or higher), of which on a minimum of three days tropical temperatures are measured (maximum temperature 30°C or higher) [KNMI, 2019]. According to Huynen et al. [2001], people who are considered healthy have an efficient heat regulation system that enables the body to cope with thermal stress. Within certain boundaries, by appropriate thermoregulatory activity thermal comfort can be preserved in a way that mental and physical activities can continue without causing harm to health. People having pre-existing medical conditions such as diabetes, mental disorders or cardio-vascular diseases are at higher risk of suffering from negative consequences caused by heat waves. Thereby, the elderly, socially isolated people, people having a low income, being uneducated, or living in low-income housing also are at greater risk [Bao et al., 2015]. Mortality as a result of unusually high temperatures has been found to be significantly higher for the elderly population [Vaneckova et al., 2010].

Thus, urbanization processes have a long-term nature, meaning that just like the climate system, decisions being made now will define the future response of the urban system. This makes climate conscious planning a vital and crucial goal [Lindley et al., 2013]. This project aims to develop a spatial risk assessment method focused on creating a heat related health risk index designed for the elderly population (aged 75 and over) which can be used to depict the vulnerable areas of the city to support adaptation strategies related to spatial planning and land use.

1.1 PROBLEM STATEMENT

The effect of the Urban Heat Island (UHI) on the health of vulnerable groups in society, especially the elderly population, has been widely recognized [Bao et al., 2015; Buscail et al., 2012; Morabito et al., 2015; Tomlinson et al., 2011; Johnson et al., 2012].

Regarding the ongoing increase of the temperature of the earth's surface together with the world's ageing society, research into the mortality and morbidity burden caused by heatwaves for the elderly population is at this point relatively sparse [Cheng et al., 2018]. In addition, more knowledge about the vulnerable groups and places in cities is necessary. In order to increase the surveillance and improve alertness when responding to events caused by heat waves the spatial detail needs to be improved. If climate risk management frameworks desire to include health and heat, information on vulnerability at spatial resolutions finer than the regional or city scale is necessary for decision makers with the allocation of resources when responding to occasions of extreme heat [Wolf and McGregor, 2013].

When studying the literature on the urban heat effect most studies do not take into account the heterogeneity of temperature measurements in a city. These studies use temperature data collected for large regions, based on weather stations often located at airports outside the city. Other studies use land surface temperature to assess the atmospheric temperature. The aim of this project is to use weather data collected by the KNMI together with datasets on socio-demographic and spatial aspects of The Hague to construct a heat-related elderly index for the city of The Hague. This index has the aim of providing more insight into the factors contributing to, and the consequences of, the UHI phenomenon. The focus area of this study is the city of The Hague (Figure 1.1). With the collected weather data from the KNMI the PET can be determined which can be used in assessing the thermal comfort of the elderly population. In combination with other spatial layers containing different indicators to assess heat stress amongst elderly, a risk index map will be generated. The aim is to develop an urban planning tool that can be used to address the health problems that are caused by the urban heat islands in Dutch coastal cities.



Figure 1.1: The municipality of The Hague [Ntarladima, 2016]

1.1.1 Scope and research questions

The harmful effects caused by extreme heat events can be prevented. Therefore, this research is focused on the development of a heat vulnerability index for the elderly population of The Hague. Because of limited time and resources, limitations are inevitable for a master thesis. Therefore, study area of the risk assessment is confined to the municipal borders of The Hague as well as temporally limited to a specific heat wave that occurred in the summer of 2018. In this thesis the focus will be on the ageing society as the vulnerable group used for creating the heat risk index for The Hague. According to estimations by Posad et al. [2018], the number of people aged 75 or over in The Hague will increase by the year 2040. Based on previously conducted research, it is widely recognized that the ageing part of the population is most effected by UHI [Kestens et al., 2011]. Therefore, it was chosen to focus on the elderly population and to exclude other parts of the population from this research. The methodology that will be applied will be based on existing

methods. Therefore, the focus is on adaptation and improvement of these existing methods in order to bring research to a next level.

Objective The aim of this thesis is therefore to add to the emerging body of knowledge related to the development of the heat risk vulnerability indexes particularly focusing on the growing elderly population residing in The Hague. This index will be achieved by making a composite map from combining socio-demographic data with spatial data.

Research question The main research question of this thesis will therefore be:

How to model the urban heat related risks for the elderly in the city of The Hague?

In order to formulate an answer to the main research question the following sub-questions will be answered:

- What are the indicators that influence the heat related health risks the elderly population is being exposed to?
- Where in The Hague is the elderly population affected the most by urban heat islands?
- What framework is most applicable for analysing the urban heat related risks for the elderly population?
- What spatial resolution is most appropriate to visualize the urban heat related risks for the elderly population?

1.2 READING GUIDE

- Chapter 3 provides the theoretical framework on which this research is based. An overview of existing methods is presented and further examined.
- Chapter 4 explains the methodology that will be used in this research. Furthermore, this chapter describes the way validation of the results will be
- Chapter 5 presents an analyses of the Netatmo sensor measurements and shows how these measurements can be used in this research.
- Chapter 6 describes the spatial layers used for composing the risk index.
- Chapter 7 presents the application of the weighting procedure.
- Chapter 9 discusses the process, results and the validation of the results.
- Chapter 8 concludes the study and provides a summary of the findings, discusses future work and recommendation, and explains the contribution of this study to geomatics.

2

THEORETICAL BACKGROUND

Now the objective of the study has been described, this chapter continues with the theoretical background on the studied topic in order to describe and understand the existing body of knowledge. First, the heatwave that took place in July 2018 is described, followed by the description of the urban heat island phenomenon. Then the concept of outdoor thermal comfort is explained along with the ways it can be expressed. Thirdly, the ways of weighting spatial layers in order to combine them in a well substantiated manner are discussed.

2.1 THE HEATWAVE OF JULY 2018

Before constructing the index, statistics on the heat wave of 2018 are discussed. The heatwave addressed in this thesis took place from the 15th of July to the 27th of July, of which the 27th was the hottest day in The Hague [Centraal Bureau voor de Statistiek, 2018]. The last heat wave that had a big effect took place in 2006, the year in which 1000 people extra died compared to a normal summer. The heatwave of 2018 took 100 extra more lives, a big difference compared to 2006 as can be seen in Figure 2.1. This difference in extra deaths can be explained by several observations.

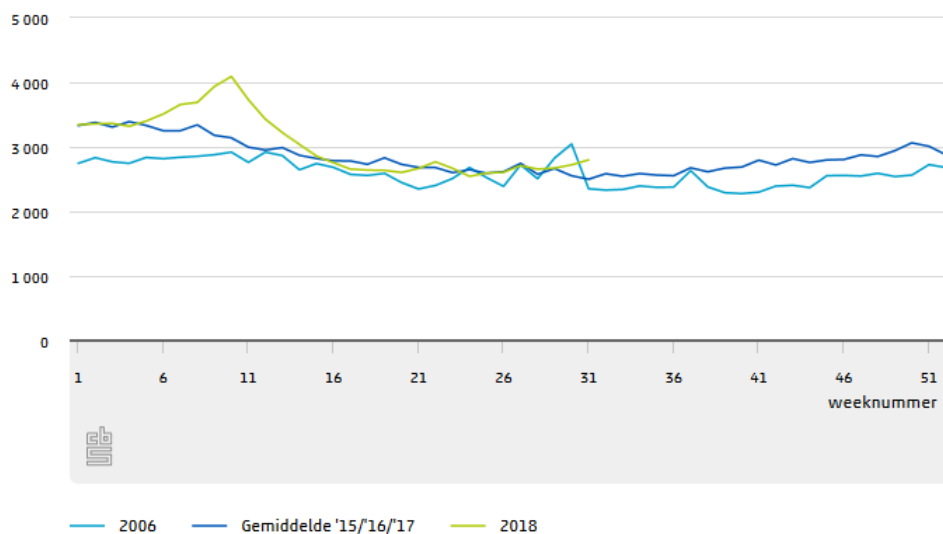


Figure 2.1: Number of people deceased per week in 2018 (in green) and of 2006 (in light blue), and the average number of deceased people of 2015, 2016, 2017 together (in dark blue) [Centraal Bureau voor de Statistiek, 2018].

First of all, according to the Centraal Bureau Statistiek (CBS) the awareness about how to act during a heat wave has increased which means that people have become better in protecting themselves from heat. Furthermore, during springtime in 2018 a flu epidemic had struck the country for a long period, which already took the life of people having weak health. Meaning that these people already succumbed before the heat wave in July came along. However, in 2018 still the elderly people were hit the hardest, as mainly people aged 80 plus died [Centraal Bureau voor de Statistiek, 2018]. Relatively the mortality rate amongst elderly during the 2018 heat

wave was lower than in 2006, however, the number was higher than in a normal summer week. During week 29 till 31 in 2018 every week on average 193 persons for every 100.000 inhabitants of 80 years and older died. In 2006 this number was during the same weeks of the heat wave (week 27, 29 and 30) at 262. In the same weeks of the summers of 2015 till 2017 183 people died every week for every 10.000 inhabitants of 80 years and older as can be seen in Figure 2.2.

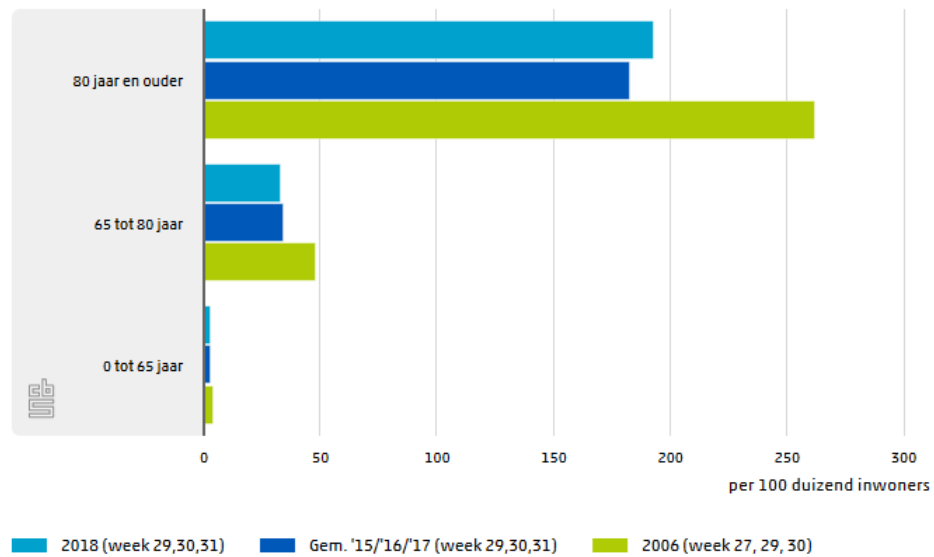


Figure 2.2: In light blue the deads in week 29, 30 and 31 of 2018. In dark blue deads in week 29, 30 and 31 of the years 2015, 2016 and 2017. And in green the deads in 2006 of week 27, 29 and 30 [Centraal Bureau voor de Statistiek, 2018].

2.2 URBAN HEAT ISLANDS

Mortalities caused by heat-related health effects take place the most in cities, a widely recognized result of the UHI effect. The UHI phenomenon comprises the observation that temperatures in cities or towns are generally higher compared to rural areas [Stone et al., 2010]. According to Van Hove et al. [2011] the differences in type of land cover, surface characteristics, and levels of human activity cause a difference in the energy budgets of urban areas. With a lack of green spaces this effect is exacerbated. The energy that is radiated by the sun and received by the surfaces of the city is equal to the energy exchanged between the air, the surfaces, the water and the vegetation [van der Hoeven and Wandl, 2018]. The energy balance of the surface can be described by the following equation .

$$Q^* = +Q_E + Q_H + Q_S$$

Q^* = The net solar radiation, obtained by the earth surface

Q_e = Latent heat flux. Energy exchanged through evaporation by water and greenery

Q_h = Sensible heat flux. (conversion of heat from the surface to air)

Q_s = Ground heat flux. Energy absorbed by the ground, buildings and surface water.

The urban atmosphere is divided into different layers as an effect of the increased surface roughness of cities as can be seen in Figure 2.3. This theoretical distinction is comprised of the planetary boundary layer (PBL) which is a part of the atmosphere that is influenced by the contact with the planet's surface. The PBL is divided into the urban boundary layer (UBL) and the urban canopy layer (UCL). The UBL is the

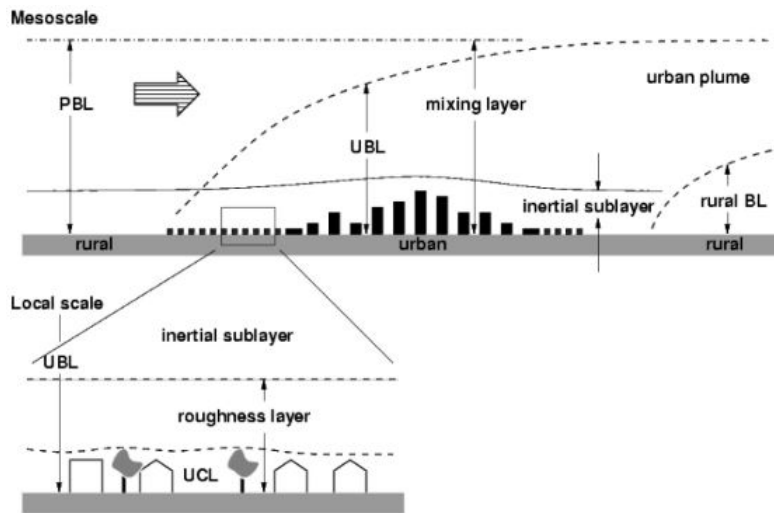


Figure 2.3: PBL, UBL and UCL [Duffy et al., 2010]

part of the atmosphere between the surface of the PBL and overlying the UCL. The UCL describes the part of the atmosphere between the surface of the earth and the tops of trees and buildings [Gunawardena et al., 2017]. The urban climate can be divided into its thermal and air quality component, where the UHI represents the characteristic of the thermal component of the urban climate within the urban canopy layer (UCL) [Mayer and Matzarakis, 1997].

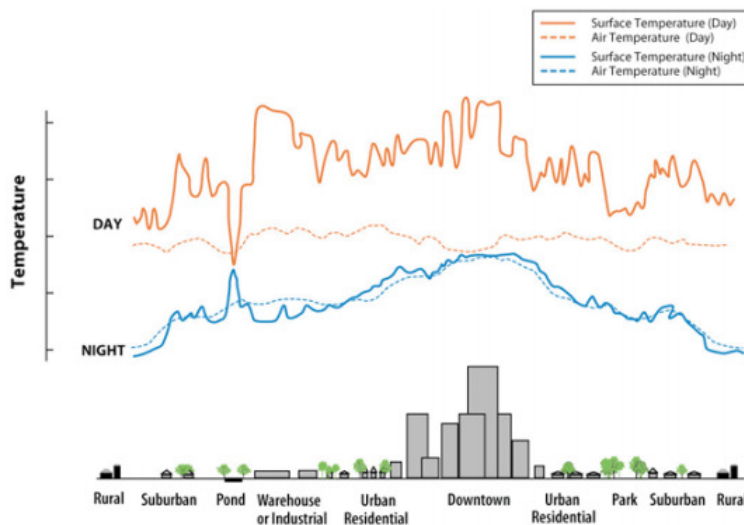


Figure 2.4: Variations of surface and atmospheric temperatures (EPA,2017)

The UHI effect identifies the distinction between the atmospheric UHI and the surface UHI [Van Hove et al., 2011] as can be seen in Figure 2.4. The atmospheric UHI is most pronounced at night after sunset and weakest during the day because of the slow release of heat from structures in the build environment. The surface UHI is both day and night present but more often the most pronounced by day when the sun is heating up the earth.

2.3 OUTDOOR THERMAL COMFORT

Due to the increase of heat stress in cities more research into thermal comfort has been conducted. The way human beings perceive the UHI is determined by their energy balance. In assessing the effect of the UHI on the health of people in a significant way, modern human biometeorology has to be taken into account. This field of study has to do with the effects of weather, climate and air-quality on human beings [Mayer and Matzarakis, 1997]. In comparison with indoor thermal comfort, outdoor thermal comfort has climatic variables that are more diverse [Honjo, 2009]. For instance, the spatial and temporal microclimatic variation of meteorological variables are usually considerable, also the person's socio-cultural and physical adaptation play a role. Furthermore, the variation among use and users of the outdoor environment and climate control being absent outside has to be taken into account [Johansson et al., 2014]. To deal with this issue the PET has been developed [Honjo, 2009]. PET is a value that accounts for the changes in thermal comfort. It is defined in literature as the air temperature at which, in a typical indoor setting (without solar radiation and wind), the energy budget of a standardised person is balanced with the same core temperature as under the complex outdoor conditions to be assessed. This standardised person can be described by a work metabolism of 80W (light activity), and by 0.9 clo (the heat resistance of clothing) [Hoppe, 1999]. The following assumptions are made for the reference indoor climate:

- The mean radiation temperature T_{mrt} is equal to the air temperature T_a .
- Wind speed is set to $v = 0.01 \text{ ms}^{-1}$.
- Water vapour pressure of ambient air is fixed at 12hPA (about the same as relative humidity (RH) of 50% at $T_a = 20^\circ\text{C}$).

This model is based on the Munich Energy-balance Model for individuals (MEMI) which models the thermal conditions of the human body in a physiologically relevant way as can be seen in equation 1 [Mayer and Höppe, 1987].

$$M + W + R + C + E_D + E_{Re} + E_{Sw} + S = 0$$

Explanation of the terms used in Eq.1:

- M = the metabolic rate
- W = the physical work output
- R = the net radiation of the body
- C = the convective heat flow
- E_d = the latent heat flow to evaporate water into water vapour diffusing through the skin
- E_{re} = the sum of heat flows for heating and humidifying the inspired air
- E_{sw} = the heat flow for cooling or heating the body

Some terms in Eq.1 are dependent on the mean clothing surface temperature T_{cl} , the mean skin temperature (sweat rate) T_{sk} and core temperature T_c . These terms are all affected by ambient conditions and or activity. Thus, to solve Eq.1 the three unknown quantities first have to be evaluated by adding two more equations. Equation two describes the heat flow F_{cs} from body core to skin surface and equation three the heat flow F_{sc} from skin surface through clothing to the clothing surface [Hoppe, 1999].

$$Eq.2 : F_{CS} = v_b \times \rho_b \times c_b \times (T_c - T_{sk})$$

- v_b = blood flow from body to core ($\text{Is}^{-1} \text{m}^{-1}$)
- ρ_b = blood density (kg/l)
- c_b = specific heat ($\text{W sK}^{-1}\text{kg}^{-1}$)

In Eq.3 the heat resistance of the clothing is expressed in $\text{K m}^2 \text{W}^{-1}$ [Mayer and Höppe, 1987].

$$\text{Eq.3} : F_{SC} = (1 \div I_{cl}) \times (T_{sk} - T_{cl})$$

In this thesis thermal comfort will be taken into account as it provides more insight in the way human beings perceive weather conditions. It is chosen to use the widely

PET (°C)	Physiological stress category
Above 41	Extreme heat stress
35 - 41	Very strong heat stress
29 - 35	Strong heat stress
23 - 29	Moderate heat stress
18 - 23	No thermal stress
13 - 18	Slight cold stress
8 - 13	Moderate cold stress
4 - 8	Strong cold stress
Below 4	Very strong cold stress

Table 2.1: PET table categorized regarding thermal stress [Matzarakis et al., 2014]

known PET value which is expressed in °C. In table 2.1 the stress categories are shown related to the PET values. For the calculation of the PET values in urban environments ENVI-met will be used. This is a micro climate model that makes it possible to calculate sunshine duration, flux densities, shadow spaces and thermal indices, among which PET. This tool is further described in section 4.8.1.

2.4 WEIGHTING AND AGGREGATION OF SPATIAL LAYERS

In order to combine different spatial aspects into one final index map, a weight has to be assigned to each individual spatial layer. In spatial risk assessment studies different approaches have been applied in assigning weights to risk criteria. Geographical Information System (GIS) based Multi-Criteria Decision Making (MCDM) is becoming one of the most used methods for spatial planning and management. It resulted in an increase of requests for supporting collaborative tools over the last decade [Chen et al., 2009]. Several MCDM methods are most commonly used in GIS environments, among which the most popular are the Analytical Hierarchie Process (AHP), Ordered Weighted Averaging (OWA), Weighted linear combination GIS [Rikalovic et al., 2014]. Furthermore, some spatial risk assessment studies use equal weighting for the combination of the spatial layers. The before mentioned methods will be addressed in this section.

2.4.1 Equal weights method

To make a heat risk index Tomlinson et al. [2011] makes use of a standardisation method to each variable on the same scale. Each individual variable is standardised by dividing it from the maximum value of that variable of the total study area. In several studies this method has been successfully applied according to [Tomlinson et al., 2011; Morabito et al., 2015; Gwilliam et al., 2006]. The argument that is

used for applying this method is ensuring the ease of combining the three layers each having a different nature. However, it can be argued that this method is too simplified, keeping in mind that the criteria are in fact of different importance.

2.4.2 Ordered weighted averaging method (OWA)

OWA is a multi criteria analyses method providing a ways of analysing, evaluating and prioritizing decision strategies. At the start, the weighting factors are not applied to specific criteria but are ordered to enable the highest criterion value to be appointed the first weighting factor [Makropoulos and Butler, 2006]. Then the second highest value is assigned to the next weighting actor, and so on. The strength of OWA is that it provides a way of efficiently generating a set of diverse solutions by changing the set of ordered weights. Moreover, OWA can generate besides a single optimal solution a combination of solutions to be analysed for developing evaluation or decision scenarios. The downside of this method is that spatial studies describe it as "global OWA" because of the implicit assumption of spatial homogeneity of OWA parameters. Therefore, the OWA approach represents spatial variability inadequately [Liu, 2013].

2.4.3 Weighted linear combination method (WLC)

This analytical method is frequently applied in GIS studies for generating composite maps, because of the ease of applying it. It is based on the concept of the weighted average. The weights of relative importance are assigned by the decision maker to each layer. Every single alternative's score is acquired by multiplying the importance weight assigned to each attribute to the alternative and then summing the products over all attributes. Next the scores are calculated for all of the alternatives and the highest of these scores is selected.

2.4.4 Analytical Hierarchy Process method (AHP)

The AHP is an application of the Weighted Linear Combination (WLC) method. Chen et al. [2009] found that the AHP method is the most popular approach in GIS studies to acquire weights for criteria and has effectively been applied to determine the relative weights of identified risk factors. The AHP method has been introduced by Saaty [2008] and is a tool that requires obtaining the weights or priority vector of the criteria. The AHP is a mathematical approach for analysing complex decision problems under multi-criteria [Malczewski and Rinner, 2015]. The AHP can be used in two distinctive ways within the GIS environment: first, it can be employed to derive the weights associated with criteria map layers, and second, the AHP principle can be used to aggregate the priority for all hierarchical levels including the level representing alternatives. The decision making process can be broken down into a process of four steps [Saaty, 2008]. First the problem has to be determined and the needed knowledge has to be gathered. Then the decision hierarchy has to be structured starting from the top level with the goal. This is followed by the level below containing the objectives from a broad perspective through the intermediate levels which are criteria on which subsequent elements depend. Ending with the lowest level that usually contains a set of alternatives, see Figure 2.5. To obtain the relative intensity of importance of the different disaster criteria based on the expert's judgement and perception, a questionnaire is most often used. Hereby each element in an upper level is compared with respect to elements in the level directly below. Then the expert judgements are put into a Pairwise Comparison Matrice (PCM) [Siddayao et al., 2014]. In the last step the priorities acquired from the comparisons have to be used to weigh the priorities in the level directly below for every element. To compare the elements, a scale of numbers how many times



Figure 2.5: Hierarchical tree structure of AHP [Siddayao et al., 2014]

more important an element is over another element with respect to the criterion is needed to make the comparisons, shown in table 2.2.

Intensity of importance	Definition
1	Equal importance
2	Weak or slight
3	Moderate importance
4	Moderate plus
5	Strong importance
6	Strong plus
7	Very strong or demonstrated importance
8	Very, very strong
9	Extreme importance
Reciprocals of above	If activity a has one of the above non-zero values appointed to it when compared with activity b, then b has the reciprocal value when compared with a
1.1-1.9	If the activities are very close

Table 2.2: Fundamental scale of absolute numbers [Saaty, 2008]

As people’s reference systems can be inconsistent, some fuzziness can be involved in the judgements of the decision makers [Siddayao et al., 2014]. A metric system has been employed to deal with this issue and determine the consistency of the results of the PCM. To determine how far the matrice is from consistency, the Consistency Ratio (C.R.) can be obtained by calculating the matrix product of the weight products and the PCM. Then the element of the resulting vector is added. Afterwards the Consistency Index (C.I.) is determined by the formula:

$$C.I. = \frac{\lambda_{max} - n}{n - 1}$$

In this equation λ_{max} represents the biggest eigenvalue and n the number of criteria. In order to determine whether the comparisons were consistent the Consistency Ratio has to be calculated:

$$C.R. = \frac{C.I.}{R.I.}$$

In this formula $R.I.$ represents the Random Inconsistency index that depends on the sample size, see table 2.3 [Siddayao et al., 2014].

N	1	2	3	4	5	6	7	8
R.I.	0.00	0.00	0.58	0.90	1.12	1.24	1.32	1.41

Table 2.3: Random Inconsistency index [Saaty, 2008]

3 | RELATED WORK

This chapter presents the literature which is related and linked to the topic of this thesis. The aim is to provide a general overview of the state of the art research into health risks caused by the UHI and specifically for the elderly society. The related work is concisely described with the goal of highlighting the gaps that this thesis is aiming to fill. It begins with a description of urban heat related studies that concern the creation of heat vulnerability index maps. It continues with studies about heat vulnerability indexes focused on elderly. To create an index map, spatial layers have to be combined into a composite map. Therefore, a section describing the ways of weighting spatial layers is included. Then, this chapter continues with a review of thermal comfort within cities, and the ways of expressing this index. It concludes with a selection of indicators representing the spatial layers regarding heat related stress for the elderly based on the reviewed literature.

3.1 REPORT ON THE HAGUE: HAAGSE HITTE

In the beginning of 2018 [van der Hoeven and Wandl \[2018\]](#) published a report on the UHI effect in The Hague as this city appeared to have the strongest heat island effect in the Netherlands. In this report the Netatmo sensor network in The Hague is used in combination with remotely sensed data. Social and spatial factors have been mapped with satellite imagery, GIS and 3D-models. In their work they found that the UHI effect in The Hague is not significantly greater than in other cities, however the effect is still considerable. Furthermore research into increased mortality among people aged 75 and over was conducted. The mortality numbers were clustered on the following aspects: dispersion of people aged 65 and over per hectare, the average age of the buildings, and the sensible warmth. No linear relation was found between the spatial dispersion of people aged 75 and the other aspects. Nonetheless, it was found there are strong spatial differences in above average mortality. The parts of the city identified to be the most problematic regarding the UHI identified are Laak, Scheveningen, and the centre of the city. In this study an extensive overview of the UHI phenomenon in The Hague has been presented. However, the report does not look into thermal comfort within the city, only land surface temperature and air temperature are considered in the maps as hazards.

3.2 HEAT VULNERABILITY INDEXES

In literature the main focus of vulnerability indexes is on floods, drought and environmental change [\[Wolf and McGregor, 2013\]](#). Since recent years, the research into HVI development has increased even though most of these studies have been conducted in the United States of America, and not in Europe [\[Johnson and Wilson, 2009; Reid et al., 2009; Uejio et al., 2011\]](#). The HVI that are reviewed in this section are all city based. The methods used to arrive at a heat vulnerability index are presented and their outcomes discussed.

3.2.1 HVI for Birmingham

Tomlinson et al. [2011] developed a heat vulnerability index for the city of Birmingham in the United Kingdom. In this study the heat-related risk for the population of Birmingham was indexed and mapped. This city has over one million inhabitants making it the second most populated city in the UK. This research uses the work of Gwilliam et al. [2006] on methods for assessing risk caused by climate hazards in urban areas as a starting point. The aim of the study was to integrate remotely sensed data with commercial social segmentation data by using a risk assessment methodology based on Crichton's triangle of risk (Figure 3.1). This research makes



Figure 3.1: Crichton's triangle of risk [Tomlinson et al., 2011]

use of the Crichton's triangle of risk, where risk is composed by three layers: the hazard layer, the vulnerable layer and the exposure layer as can be seen in Figure 3.2. Tomlinson et al. [2011] distinguishes the vulnerable population into five groups: the elderly people, people with ill health, people living in densely populated areas and people living on the top floor or in high rise buildings. Firstly, the risk layers are

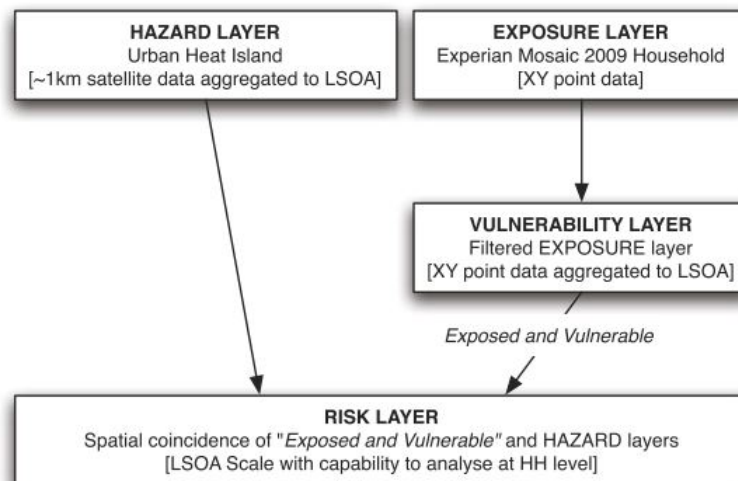


Figure 3.2: Workflow of the GIS spatial risk assessment methodology used to assess Birmingham [Tomlinson et al., 2011]

defined and afterwards a more detailed analyses can be performed down to the household level. The gaps in this research are that it uses LST as temperature measurements, which differs from air temperature. Moreover, the verification of the results is hard to establish as it is hard to measure the health of the citizens.

The HVI studies look in general at the multiple groups within the city. Few studies look into a specific part of the population to create a vulnerability index for Morabito et al. [2015]

3.3 MAPPING OF HEAT-RELATED RISKS FOR THE ELDERLY IN ITALY

Several major Italian cities have been researched by [Morabito et al. \[2015\]](#) on the heat related risks for the elderly population. In this research the workflow pictured in [Figure 3.3](#) was used to construct heat-related urban risk maps regarding elderly people aged 65 and over. This work flow is based on the layer based risk analyses developed by [Tomlinson et al. \[2011\]](#). According to [Morabito et al. \[2015\]](#), temperature is the main social-demographic indicator of heat exposure to the vulnerable population usually used in risk assessment studies. The weighting of the layers is kept equal in order to prevent manipulation and keep transparency in the process. The hazard layer is comprised of the LST which is derived via remote sensed data and weighted at 50% in the work flow. The vulnerability layer consists of the el-

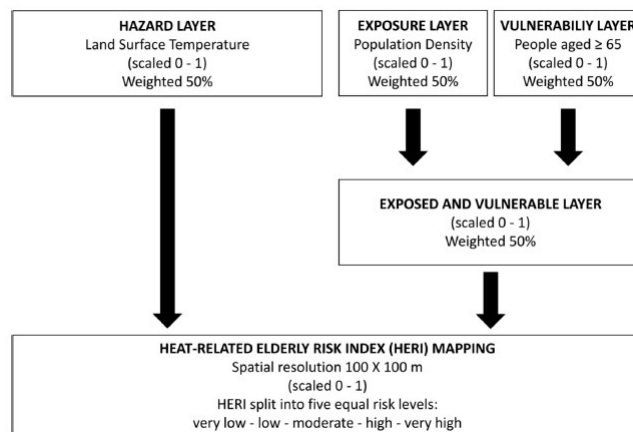


Figure 3.3: Morabito workflow [[Morabito et al., 2015](#)]

derly society as it is vulnerable to heat the most because of physiological, health and socio-economical status according to [[Morabito et al., 2015](#)]. The exposure layer is comprised of the population density, and together with the vulnerability layer the exposed and vulnerable layer is formed, together weighted at 50%. For the final mapping of the [HERI](#) the exposed and vulnerable layer is combined with the hazard layer. It creates an index in five equal risk levels: very low, low, moderate, high, and very high. This study provides a method for the urban heat risk indexing for the elderly population, by developing a clear layer based work flow. The limitations in this study are that the LST is used in the hazard layer for potential population exposure, as the relationship between LST and ambient temperature is complex. Also, the vulnerable layer is composed of the elderly population and the exposed layer of the population density. No other socio-demographic variables have been taken into consideration. Furthermore, in combining the layers each layer has the same weight assigned to it making every layer equally important. This decision lacks an explanation.

3.4 SOCIAL DETERMINANTS OF HEAT VULNERABILITY

There are a multitude of vulnerability determinants to heat for human beings. In the study conducted by [Arup \[2014\]](#) the aim of the project was to identify and explain the factors contributing to the risks caused by urban heat and to map these factors in order to visualise with using, where possible, available data. With these visualisations and maps, adaptation approaches and responses have been developed. Three categories regarding factors contributing to the [UHI](#) have been identified, called the "triple risk index" as can be seen in the [table 3.1](#). This research clearly defines the

UHI risk factor	Explanation
Location within London	-Proximity to a UHI (hot spot) like a dense building area, a major road junction -Proximity to a cool spot such as a park, water body -Levels of air pollution, noise, crime and socio-economic deprivation
Characteristics of building	Building age, materials, orientation, layout, height, storeys, deep plan, dual aspect, balcony, garden, thermal mass, shading levels and ventilation
Characteristics of people	Health, age, mobility, sex, socio-economic status, culture, languages spoken, heat risk awareness and perception, social connection level

Table 3.1: Triple index [Arup, 2014]

factors of heat risk and provides a good bases on which future research into urban heat risk can build. Nevertheless, a missed opportunity in mapping the urban heat risk is that no index has been created which relates the risk factors to the air temperature data.

3.4.1 Loneliness amongst the elderly

The social conditions of elderly people have an effect on how they live through events of extreme heat. This became already clear during the heat wave in Paris in 2003, in which there where 15000 excess deaths particularly among elderly aged 75 and over [Gusmano and Rodwin, 2010]. The elderly are especially at risk, as the result of a potential decrease in social contacts and the physical effect elderly age has on thermoregulation [Basu and Samet, 2002]. Tomassini et al. [2004] states that social isolation has been identified a key indicator during heat waves and immoderate heat events in general, especially for the elderly population. When people live alone and have possibly fewer social connections which can lead to increased vulnerability and in time dead.

3.5 SPATIAL DETERMINANT OF HEAT VULNERABILITY

3.5.1 Indoor temperature and the orientation of the facade

The relation between indoor thermal comfort and facade orientation has been described in literature where most studies focus on the combined impact of the shape of the building, the window to wall ratio and the orientation of the building. According to Ali-Toudert [2007] the urban canyon can be divided into two parts: street level and building part as can be seen in Figure 3.4. By implication, the street form affects the thermal sensation of people as well as the global energy consumption of urban buildings [Ali-Toudert, 2007]. The orientation of the facade has an impact on the solar gain inside the building. The geometry and orientation of the street canyon have an impact on outdoor and indoor environments, solar access inside and outside the buildings, the permeability to airflow for urban ventilation, as well as the potential for cooling of the whole urban system Shishegar [2013]. A buildings orientation affects the energy and comfort implications of solar shading, window to wall area ratio, performance and position of windows, and the exterior colour of the building [Bicol et al., 2009]. In research on climate change adaptation measures for residential buildings, conducted by Porritt [2012] it is stated that terraced houses have a much larger spread between minimum an maximum number of overheating than detached houses. This can be explained because two of the four sides

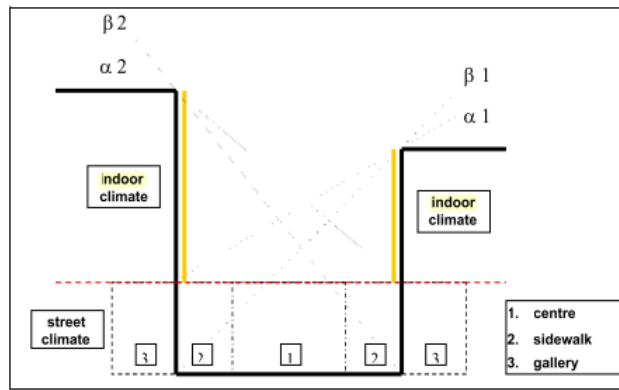


Figure 3.4: Subdivision of street canyon according to climatic design needs[Ali-Toudert, 2007]

in a terraced house are exposed to solar radiation among other ambient conditions. The orientation of a terraced house affects the number of overheating hours significantly. In case the front facade is orientated east or west this means that about two times the number of overheating hours and degree hours is present compared to the north and south orientation of the front facade, which indicates the strong effect of building orientation for the terraced house. According to Williams et al. [2019] health impacts from extreme heat are researched mostly through ambient meteorological measurements which results in exposure misclassification as buildings change indoor temperatures and ambient temperatures are not uniform throughout cities.

In his study Williams et al. [2019] conducted an assessment on adaptive behaviours of elderly during heat waves. Individual temperature exposures at home and thermal comfort, indoor environmental quality using personal sensors and wearable devices were characterized. Moreover, environmental and behavioural indicators influencing resilience and adaptive capacity during extreme heat events, which influence an individual's susceptibility to poor health outcomes during an extreme heat event. The research showed that indoor temperatures affect people's physiology. At the same time, the way participants perceive the temperature indoor and the impact of these exposures on their activities and sleep worsened. However, older people (older than 65) despite the thermal decomposition, even during non severe heat waves, do not apply adaptive behaviours enough such as hydrating enough during the day [Williams et al., 2019].

3.6 VALIDATION OF HEAT RISK MAPS

An important part of the development of risk index maps is validating them by confronting the results with observational data and by testing the results. In past researches different approaches have been applied. Bao et al. [2015] describes these applications in his review of HVI.

Maier et al. [2013] determined for the HVI of Georgia whether the extremely hot days had greater mortality rates than days that did not have dangerous temperatures. They also established if countries with higher vulnerability depicted by the HVI, had higher death rates on dangerously hot days than on days having normal temperatures. It was found that when the vulnerability increased also the relative risk of mortality increased. In some regions extremely hot days lead to a 7.7% increase of the death rate.

Wolf and McGregor [2013] calculated first the categorical statistics and related skill scores in the situation where either above average mortality or ambulance call-out happened or not. Then by applying Poisson regression analyses it was looked to

what level the relative risk of the said health outcomes changed with an increase in heat vulnerability. Thirdly, an independent samples test was carried out of the difference of ambulance call-out and mean mortality between census units having or not having high heat vulnerability and exposure. As a result the HVI provided a potential as a priori factor of the degree of mortality and ambulance call-out during summer days and heat wave events [Bao et al., 2015].

Reid E. et al. [2012] researched whether higher rates of morbidity and mortality occurred in the areas depicted by the HVI having a higher heat vulnerability on the oppressively hot days. The interaction of the HVI and deviant days on the mortality and hospitalization counts was modelled. Deviant days where the deviation of the maximum temperature from the 30-year normal maximum temperature is above or equal to the 95th percentile [Bao et al., 2015]. It was found that on both normal and deviant days the HVI was associated with higher mortality and hospitalization rates [Bao et al., 2015].

Vulnerability [2015] constructed a HVI at the census tract level with which he could predict the hospitalization of heat-related diseases based on the method of [Reid et al., 2009] who developed a method for the HVI assessment on a national level. It was found that the HVI had an overall accuracy rate of only 54% in predicting heat-related outcomes. They suggested more indicators should be included in the composition of the HVI to predict better. Furthermore, it was found that the HVI performed better in predicting non-vulnerable areas than vulnerable areas.

4 | METHODOLOGY

This section addresses the research questions and will provide an overview of the steps that are taken to complete the different phases of the research. In Figure 4.2 the methodology flowchart is shown.

4.1 LITERATURE AND RELATED WORK REVIEW

In this first step a thorough literature review has been carried out in order to find out what has been done and to determine the knowledge gaps. The reviewed literature has provided an overview of the definition of the UHI and gave insight into the factors that contribute to the vulnerability of the elderly population of urban heat. Furthermore, it has brought forward the ways of assessing and visualising the urban heat risks. In addition, the technological and terminological foundation of the thesis has been provided.

4.2 SENSOR DATA RETRIEVAL, STORAGE, CLEANING AND ANALYSES

The atmospheric data gathered by the [KNMI](#) will be collected for the summer period of 2018. As the [KNMI](#) data is already stored and freely available on the internet, it is easily accessible and ready for use. Furthermore, in order to work with the sensor measurements collected by the Netatmo sensors, these have to be retrieved and put into a spatial database. In total the database contains the large amount of 14.688 files for the period of May 2018 up to end September 2018. Thereafter the data can be cleaned from outliers and analysed. With the spatial database specific days from the summer of 2018 be retrieved and used for further analyses.

4.3 COLLECTION, AGGREGATION AND ANALYSES OF ADDED SPATIAL DATA

The next step is to collect the spatial data needed for modelling the urban heat related risks for the elderly population. Firstly, the spatial risk assessment method has to be defined. The primary risk assessment theory of this work is build upon Crichton's Risk Triangle that describes risk as a function of three components: hazard, exposure and vulnerability, that must be spatially coincident in order for risk to exist. When one of the components yields zero, no risk exists. Furthermore, the factors contributing to the risk have to be defined. To be able to include the indicators, the data about them has to be measurable, freely available and accessible. In this thesis the risk components have to be translated into a fitting layer-based structure appropriate for analyses in a GIS-environment.

4.4 DEFINING THE SPATIAL LAYERS

This study will be built upon the methodology that was developed by [Morabito et al. \[2015\]](#) that concerns the [HERI](#). In order to make a composite index map of different spatial layers the indicators representing the layers have to be defined. Important is that the different layers are not related to each other and do not explain each other. There are six indicators that are used to represent the spatial risk layers: [PET](#), indoor temperature, being 75 years or over, loneliness amongst 75 years olds, population density, and facade orientation.

4.4.1 Hazard layer

The hazard will be represented by the [PET](#) and the indoor temperature. For modelling the [PET](#), the tiles from the Vierkantstatistiek 100m dataset will be selected having more than zero elderly people living there. The areas of the Vierkantstatistieken 100m tiles will be modelled with the aid of ENVI-met software. Weather data collected by the [KNMI](#) weather station is used as an input for the micro-climate software ENVI-met (this software will be described in section [4.8.1](#)). In addition, the hazard to which the elderly are exposed is also represented by the indoor temperature in a residential house. This indicator presents on the neighbourhood level what the average temperature within houses was during certain moments of the day. People spend the main part of the day inside where they are exposed to the temperature inside. For this reason two indexes will be created with one having [PET](#) as the hazard and the other index having indoor temperature as hazard.

4.4.2 Exposure layer

The exposure aspect represents what is exposed to the hazard. Basically it is a simple coincidence between the hazard and the exposure of interest [[Tomlinson et al., 2011](#)]. There are various components that can be exposed to the hazard for which relevant spatial data about every component is required in order to be useful. For instance people could be exposed to a hazard, with related meta data available on age or health issues. Furthermore, buildings could be used as exposed element by looking at age type indoor temperature or orientation of the buildings [[Tomlinson et al., 2011](#)]. The exposure layer in this thesis will be represented by the population density as a socio-demographic indicator which can be retrieved from the Vierkantstatistieken 100m tiles containing socio-demographic information. Moreover, the facade orientation of a building will be looked into as an indicator of exposure. The facade of a house is exposed to the direct radiation from the sun affecting the temperature inside the house. However, because the facade orientation directly influences the indoor temperature these two indicators can not be used in the same index, as it is not allowed for two indicators to explain each other. Therefore it is chosen to see how these indicators are weighted and thereafter put into a separate index from each other. Then it is looked how every index scores on explaining the heat related health risks of the elderly population.

4.4.3 Vulnerability layers

The vulnerability of people to heat depends on one hand on climatic risk factors such as the frequency of heat waves, and on the other hand on individual risk factors being the gender, age, medication use, disease, hydration level, living alone, and the housing situation (building type, residing on a higher floor) of the person. Furthermore having an air conditioning and making use of it is part of the individual factors [[Tan, 2008](#); [Arup, 2014](#); [Morabito et al., 2015](#)].

As vulnerable population the elderly population (aged 75 and over) is defined,

which is retrievable from the Vierkantstatistieken 100m tiles. Furthermore, an additional vulnerability layer containing the social component loneliness, is added to the framework. These aspects of the built environment influence the vulnerability of the elderly will be represented by the orientation of the facades.

The indicators are stated per layer in the workflow shown in Figure 4.1 which is based on the work flows developed by Morabito et al. [2015]. The defined weighted layers are used to generate the HERI maps that aim to indicate the risk areas for the elderly population of the city of the Hague in times of extreme heat events.

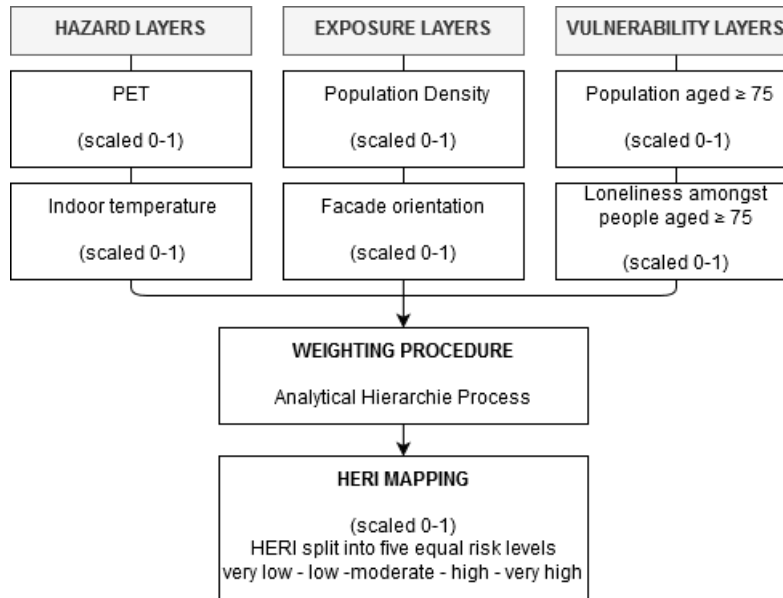


Figure 4.1: Workflow, based on Morabito et al. [2015].

4.5 WEIGHTING PROCEDURE

The composition of the heat related health risk index for the elderly population consists of three layers: the hazard layer, the exposure layer and the vulnerability layer. The three layers are each of a different nature and contain criteria of different importance. Therefore a method is selected for combining the layers into to one composite map. In spatial modelling for risk assessment the mathematical AHP method has effectively been applied to determine the relative weights of identified risk factors, with the use of expert opinions. To obtain these opinions about the relative importance of the factors with regard to the impact on the vulnerability of the elderly population, a questionnaire has been put together. Through this questionnaire the relative impact of the criteria on vulnerability to heat for the elderly population will be determined through expert opinions. Then the PCM can be executed for obtaining the weights of the six indicators, followed by a consistency check.

4.6 MAPPING HERI

To create the HERI maps the hottest days of summer 2018 are selected from the data collected by the KNMI sensor in Hoek van Holland. As the software needs starting up time meaning that the first hours for which it simulates are not accurate multiple days have to be simulated in order to retrieve valid outcomes. Therefore the days of the 26th to the 28th of July have been chosen to get accurate calculations for the 27th of July. This calculation takes ENVI-met around 24 hours for a 100 by 100 meter

area. Therefore locations within The Hague will be selected based on the spatial distribution of people aged 75 and over in order to determine whether the elderly live mostly in hazardous areas regarding urban heat islands that will occur more in the coming years with increasing temperatures due to climate change. For the hottest day three moments will be selected: 04.00 o'clock, 14.00 o'clock, 24.00 o'clock (as the UHI is a nocturnal phenomenon). These moments will be indexed and put into a map. The hazard, exposure and vulnerability layers will be individually mapped before mapping the **HERI**. The mapping of **HERI** will create maps indicating heat related risk for the elderly population indicated on a scale ranging from very low, low, moderate, high, to very high risk.

4.7 VALIDATION

In mapping of urban heat vulnerability it is widely known that validation of the results is an important component. The mapping of **HERI** will create maps indicating heat related risk for the elderly population on a scale ranging from 'low risk' to 'very high risk'. In order to check whether the mapping of **HERI** yields valid results, the number of deceased elderly people (age 75 and over) in The Hague after the heat wave will be used for validating the results. It will be checked if the number of deceased people in a certain area is higher when the risk in that area also is greater compared to other areas. The significance of the results can then be determined.

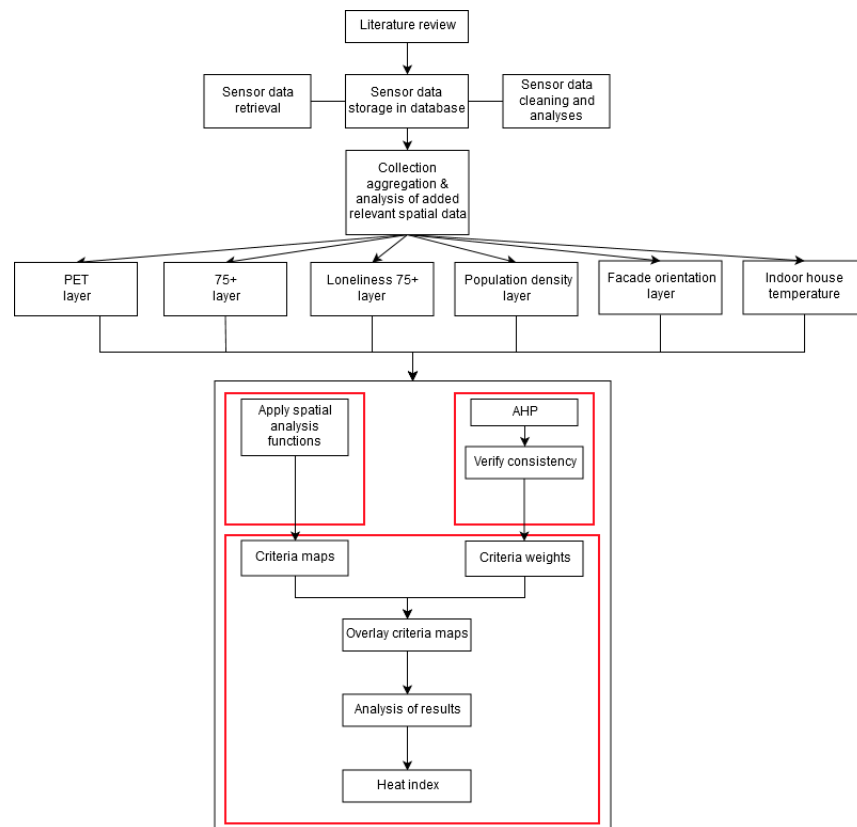


Figure 4.2: Methodology research

4.8 TOOLS AND DATASETS

4.8.1 Tools

This section presents the tools that will be needed in this research in order to process, analyse and manipulate the gathered data. An elaboration on how they were used can be found in chapter 6.

- Python

As programming language Python provides libraries such as 'psychopg' and 'datetime' that can be used for creating the spatial database to store weather data. Another reason for using this specific programming language is familiarity and it being a freely available software.

- PostgreSQL database

This is an open source software that has support for geographical data due to the PostGIS extension that provides spatial data processing capacity. It is used in this project for storing the weather measurements conducted by the Netatmo sensors as can be seen in figure 4.3. This type of database will make it possible to clean the data by removing outliers from the dataset. Afterwards the data can be used for analyses in software like QGIS.

measure_id ▲ [PK] double precision	sensor geometry	date date	time time without time zone	mac text	altitude double precision	temperature double precision	humidity double precision	rain_50min double precision	rain_24h double precision	pressure double precision
1	1	0101000020E61...	2018-... 00:00:14	70e...		1	7.1	81	0	999.3
2	2	0101000020E61...	2018-... 00:00:14	70e...		3	7.2	92	[null]	1002.2
3	3	0101000020E61...	2018-... 00:00:14	70e...		3	7.5	94	1.111	23.634
4	4	0101000020E61...	2018-... 00:00:14	70e...		11	7.5	94	[null]	997.5
5	5	0101000020E61...	2018-... 00:00:14	70e...		4	7	97	0.606	21.109
6	6	0101000020E61...	2018-... 00:00:14	70e...		1	7.5	91	0.404	23.634
7	7	0101000020E61...	2018-... 00:00:14	70e...		1	7.3	92	0.505	0
8	8	0101000020E61...	2018-... 00:00:14	70e...		3	7.5	93	0.505	21.917
9	9	0101000020E61...	2018-... 00:00:14	70e...		4	[null]	[null]	[null]	999.5
10	10	0101000020E61...	2018-... 00:00:14	70e...		2	8	91	[null]	1000.1

Figure 4.3: Database containing the Netatmo measurements in PostgreSQL

- Quantum Geographical Information System (QGIS)

For data visualisation QGIS will be used. This is an open source geographical information system which is freely available. It enables spatial data processing, analysing and mapping which will makes it an essential tool to use in this thesis to process the weighted layers described in the workflow.

- ENVI-met

This is a three-dimensional non-hydrostatic model which will be used to calculate the PET values. This tool is used in the applied climatology field to simulate micro-scale thermal interactions within in urban areas [Hien et al., 2012]. ENVI-met uses both calculations having fluid dynamics characteristics among which turbulence and air flow, thermodynamic processes happening at roofs, ground surface, walls and plants. Figure 4.4 shows the simplified layout used for modelling in ENVI-met. Furthermore, direct, diffused and reflected solar radiation are taken into account when calculating the mean radiant temperature. Different tools exist within the ENVI-met software: Spaces, Biomet and Leonardo. The Spaces tool can be used to model the area of interest. This model was selected for its capability to simulate the urban micro-climate whilst dealing with a broad range of factors which include the vegetation, complex building shapes, land cover materials and building material. With this tool the buildings, streets, including building materials. Furthermore, the vegetation such as grass, plants can be modelled and types of trees can be specified. The PET is calculated using the Biomet tool. The parameters for the PET calculation that can be adjusted include: sex, age, weight, static clothing insulation, and work metabolism, as can be seen in Figure 4.5. Based on the

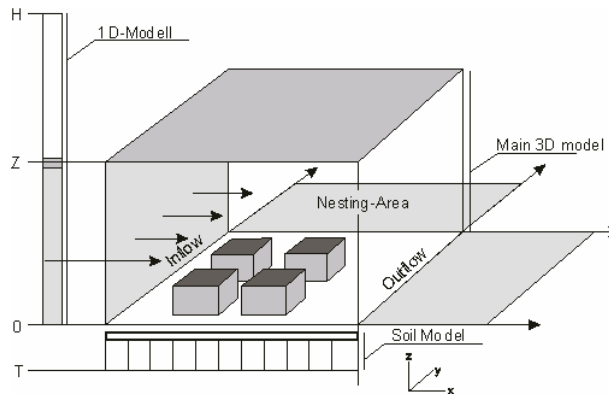


Figure 4.4: Simple layout of ENVI-met's fluid dynamics model [Rosheidat et al., 2008].

Figure 4.5: The human parameters that can be adjusted in the Biomet tool for calculating PET values.

Gagge-2-node model the skin and core temperature are related which is generated by the outdoor environment to the indoor air temperature which results in the same temperatures. For visualisation of the maps a tool called Leonardo can be used. Within this tool the simulated data output is loaded. The table of content contains several layers: data layer, special layer, vectors and particles, contour layer and the symbol layer. The software comes with some limitations

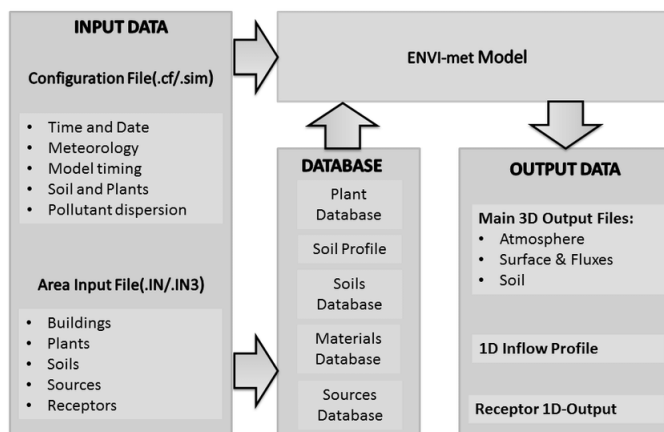


Figure 4.6: Data flow within the ENVI-met environment [Maleki et al., 2014].

that have to be taken into account. The maximum spatial resolution of ENVI-met is set at $250 \times 250 \times 25$ grids because of the great computational force that is needed to run the simulations. Furthermore, the attributes available

to construct the micro-climate models are buildings, soil/pavement materials and trees and vegetation. It is not possible to create other object such as shade structures aside from the buildings. The buildings in ENVI-met only have one single constant temperature and no thermal mass. In addition it is not possible to simulate moving water bodies as the water bodies are put in as a soil profile[Rosheidat et al., 2008]. When choosing a duration span in which i simulated ENVI-met does not allow the user to take more than 2 nights of simulating.

- Statistical Package for the Social Sciences (SPSS)
This software is used by wide range of researchers for complex statistical data analysis. It is used for statistical analysis and data management. In this thesis it is used to calculate correlation coefficients in order to perform a test of validity on the results of this research.
- Haagse Bomen App
This online database contains the trees planted in the streets of The Hague. Figure 4.7 shows the interface of the app, in here the tree of interest can be selected retrieve information about the scientific name, Dutch name, age and stem diameter category. The legend provides information on the trees in the map in general to see the age category of the trees, whether it is an monumental tree and if the tree is planted in a forest or in a plantation. Information about the tree species will be used for choosing the correct tree when modelling the urban areas in Envi-met.

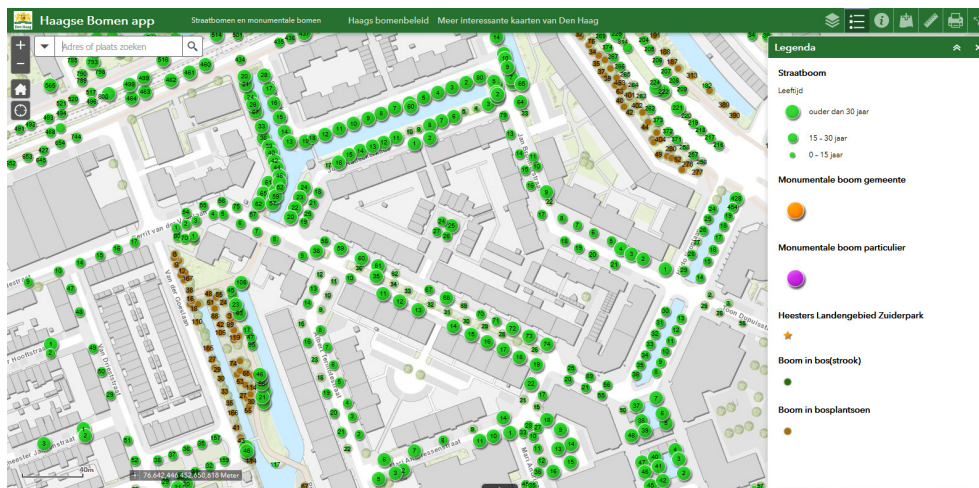


Figure 4.7: Interface of the Haagse Bomen App

4.8.2 Datasets

The following datasets will be used in the research.

- KNMI weather data
This is data collected by the KNMI weather station in Hoek van Holland (Zuid-Holland). It exists of files ordered by timestamps providing information temperature, rain for the past hour and of the last 24 hours, humidity and pressure. With regard to calculating PET, information about rain of the past hour and last 24 hours will not be included in the research.
- Netatmo weather data
This is data collected by the Netatmo sensors provided by the TU Delft. It exists of files ordered by timestamps providing information about the position

and altitude of the specific sensor and measurements including temperature, rain for the past hour and of the last 24 hours, humidity and pressure. The spatial extent of the dataset includes also cities such as Rotterdam, Leiden and Zoetermeer. However the focus area of the study is the municipality of The Hague meaning the sensors in these cities will be excluded from the research.

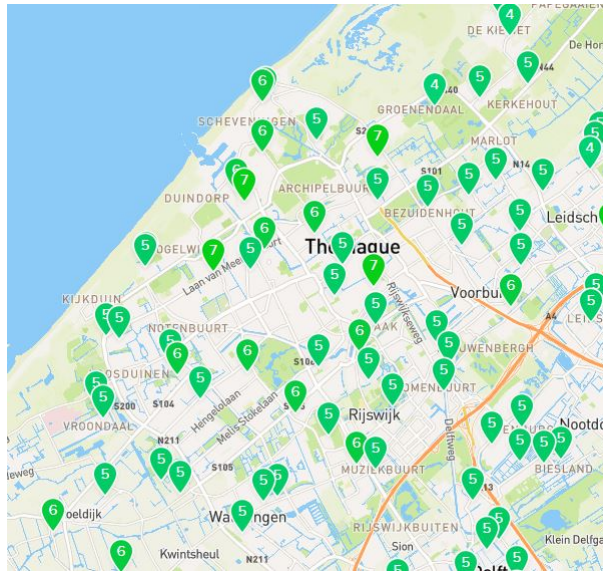


Figure 4.8: Netatmo sensors

- CBS Vierkantstatistieken 100m
This map has a grid structure of 100 by 100 meter containing socio-demographic information on the population. This dataset includes information about: amount of inhabitants, number of inhabitants clustered by age, origin of the inhabitants, households, income, energy use, social security and building information. This dataset is freely accessible from the PDOK service.
- Data on mortality
Data concerning the total amount of people that died and the mortality amongst people aged 75 or over in The Hague during the summer of 2018. The map is constructed of 100 by 100 meter tiles.
- Algemeen Hoogtebestand Nederland (AHN)
The AHN is a digital height map of the Netherlands. It provides detailed and exact heights which the user can obtain through a web viewer. It contains an average of eight height measurements for every square meter.
- Rijks Instituut voor Volksgezondheid en Milieu (RIVM) map on loneliness amongst elderly
This map contains information on the percentage of elderly people that are feeling lonely/ extremely lonely mapped for every neighbourhood.
- Open Street Map (OSM)
A freely accessible web service that provides roads, cycleways, footpaths etcetera. The wanted tiles can be downloaded from the website to use in QGIS.
- Indoor temperature measurements from Quby sensors
A dataset containing the indoor temperatures of houses in The Hague that own a Quby sensor. The data is aggregated on the neighbourhood level. In the dataset the average temperature, the standard deviation of temperature for every every hour is presented. In addition, the amount of users of the sensor are gathered for the summer of 2018.

5 | SENSOR DATA

In this section the data coming from two types of sensors will be discussed, Netatmo sensors and Quby sensors. First the data from Netatmo sensors will be discussed. In total there are 249 Netatmo sensors within the borders of the municipality of The Hague. Each sensor collects atmospheric data every 15 minutes, providing a complete overview on the behaviour of the weather in The Hague. From this data it can be seen when The Hague went through a heat wave. This chapter looks into the days on which the most tropical temperatures were measured. Further, it investigates the parts of The Hague that are the hottest during these tropical days. To conclude, it is explained and decided whether to use the Netatmo sensors in this research or not. Then it will continue with data coming from Quby sensors which are installed inside homes to measure the temperature.

5.1 TROPICAL DAYS

In diagram 5.1 the amount of times per day that sensors in the Hague measured temperatures above 30°C is displayed. Six peaks can be read from the diagram during which the sensors measured temperatures crossing the 30 degree mark. The highest peak is on the 27th of July when the Netatmo sensors measured 10302 times temperatures above 30°C. This day was according to the data the hottest day of the summer of 2018.

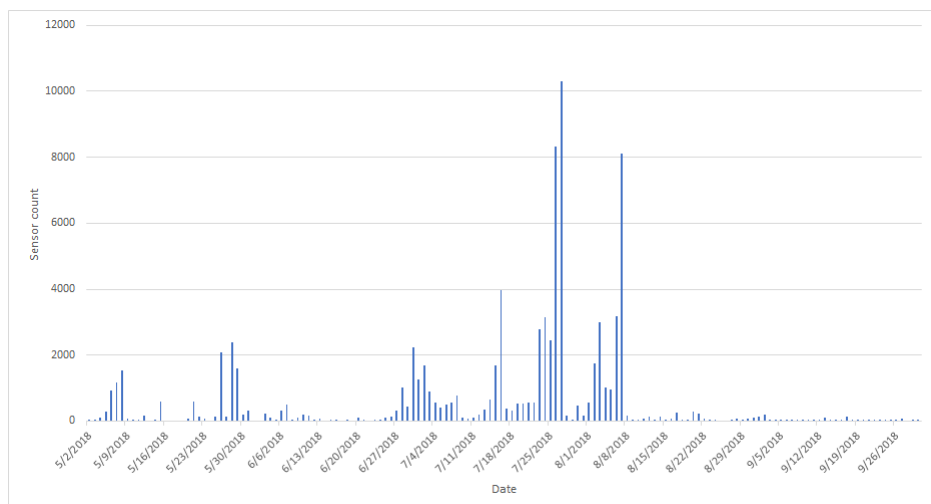


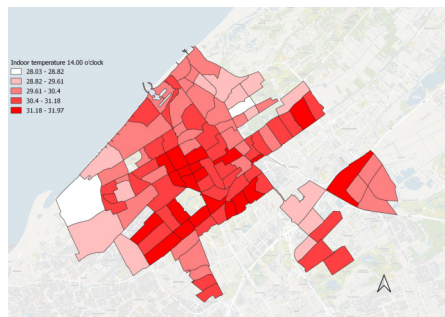
Figure 5.1: Diagram depicting how many times the sensors have measured temperatures above 30 °C for each day over the period 05/02/2018 till 09/30/2018.

5.2 USING THE TEMPERATURES TO VALIDATE THE ENVI-MET MODELS

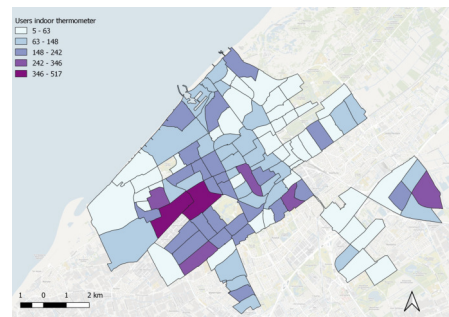
With the ENVI-met tool, nine locations within The Hague have been modelled. It would be very convenient to interpolate the measurements and create a map on a certain time from both the calculated ENVI-met temperatures as the Netatmo sensor measurements. However, it is not known what the specific location of the Netatmo sensors is. This accuracy can vary for every sensor, therefore making it hard to accurately validate the ENVI-met simulations. Further, it is not known what the conditions are in which the Netatmo sensors are put. For example, it makes a great difference if the sensor is placed in a shadowed spot or in a spot that receives sunlight throughout the day. For these reasons it was chosen to not use the Netatmo sensors for validating.

5.3 QUBY SENSORS

The temperature data coming from Quby sensors provides information on temperature measured inside people's homes. Where in the homes the sensor has been placed is unknown. The data is aggregated on the neighbourhood level and covers the months July and August of 2018 and 2019. For every neighbourhood the average temperature is given in degrees Celsius together with the standard deviation of the temperature, and the amount of users of Quby sensors. In Figure 5.2a the map for the timestamp 14.00 o'clock in the afternoon on 27th of July 2018 is shown as an example of how the map looks like. In Figure 5.2b the amount of users in every neighbourhood is displayed. This dataset is used as an indicator of exposure but also as an indicator of hazard as is explained in sections 4.4.1 and 4.4.2. By aggregating the data on the neighbourhood level the privacy of the users is kept safe. It is also not known where inside the houses people have put their Quby sensor.



(a) Indoor temperature at 14.00 o'clock on 27th of July 2018.



(b) The amount of users of the Quby sensor for every neighbourhood in The Hague.

6

PREPARATION SPATIAL LAYERS FOR THE INDEX

In this chapter the spatial layers used for composing the risk index map are discussed. For every layer the preparation and composition is discussed next to the dataset and tools that have been used. Every layer is first created and analysed before it is used for constructing the composite index map. To make a composite index map, each layer is transformed to a grid with 100 by 100 meter tiles in order to be able to overlay them. The location 'Weesperstraat' is used as an example to work through the different steps. The maps that were created for the indicators can be found in the appendix.

6.1 HAZARD LAYER: PET

This study was carried out in the city of The Hague (coordinates 52.0705°N , 4.3007°E) which has an oceanic climate according to the Köppen–Geiger classification. Dominated by the polar front throughout the whole year, this climate has to changeable often overcast weather. A characteristic feature of the oceanic climate is that it has soft summers, however hotter, stable weather patterns can set in for periods of time [Peel et al., 2007]. From the data collected by the Netatmo sensors in combination with the KNMI measurements it could be concluded that the days of the 26th and the 27th of July were the hottest days for the city of The Hague during the summer of 2018. To assess the thermal comfort the PET values represent the hazard layer. Weather data from the KNMI has been used as input for the ENVI-met microclimate model. In order to calculate the PET values for the whole city of The Hague first nine locations in The Hague have been selected first to model the micro-climates. Then with the use of the Biomet tool the PET values can be calculated for every location. The PET is afterwards interpolated over the city to create a PET map.

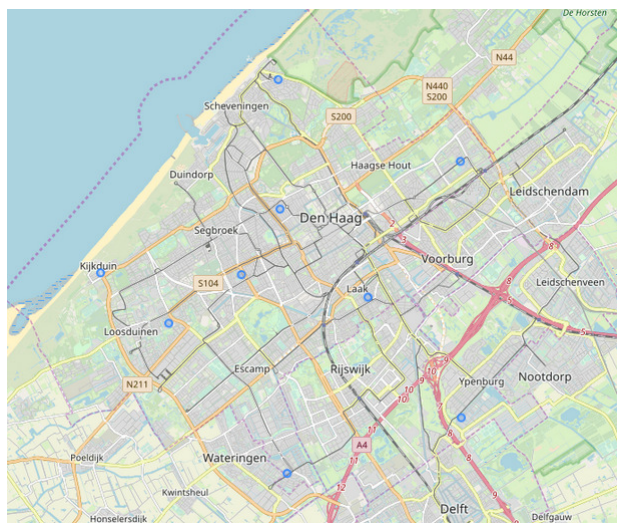


Figure 6.1: Map containing the nine locations (in blue dots) throughout The Hague where the PET values have been calculated.

6.1.1 Selection of the locations

ENVI-met was not developed to be used for modelling whole cities, as it was developed to model micro-climates within a city. Therefore, it is chosen to pick and model nine locations within The Hague. These locations are based on the tiles of the Vierkantstatistiek 100m dataset. The nine tiles are spread equally over The Hague in order to cover the whole city. Furthermore, the tiles contain information about the number of people aged 75+ and the population density. It was made sure that each selected tile contained elderly people. Table 6.1 contains the streets of the locations together with the number of 75+ year old living within that 100m Vierkantstatistiek tile. Figure 6.1 shows the spread of the locations over the city. With the Spaces tool that is available in ENVI-met, models of the locations were constructed that include the buildings, streets, trees and the materials present at the sites.

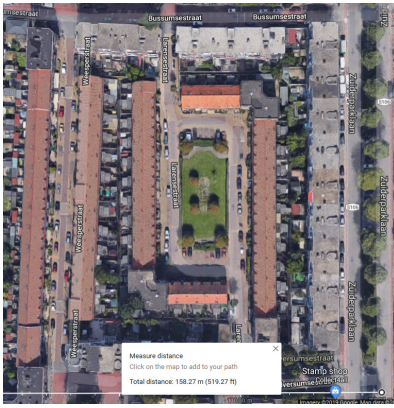
Street	Nr. of inhabitants	Nr. of people aged 75+
Gerrit van der Veen laan	35	35
Boschestraat	280	35
Tasmanstraat	170	20
Weesperstraat	195	40
Westkapellelaan	90	50
Johan Gramstraat	255	15
Zwedenburg	140	35
Athenesingel	105	25
Rijswijkse Landingslaan	130	25

Table 6.1: The selected locations in The Hague together with the amount of people and elderly living in the selected 100m tile.

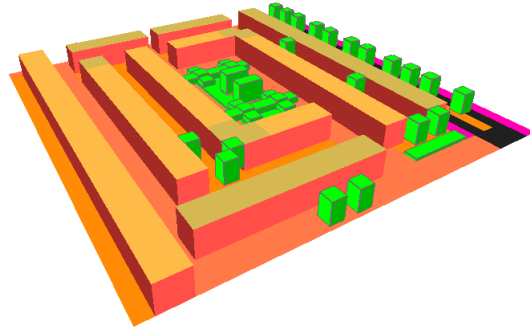
6.1.2 Simulation set-up

For the simulation of the urban micro climates, ENVI-met requires a spatial description of the test area and four (standard) databases containing thermal and hydrological properties of the surfaces and materials present in the area. The file describes the spatial configuration of the test area, the location and the height of the objects in the area. Furthermore the wall material and roof material are stored. In addition, the location, type and height of vegetation (trees, lawn) must be specified, as it is the surface material and soil type of non-built surfaces. The models of the nine locations are based on digitized images taken from Google Maps. The areas then could be built with the Spaces tool. For modelling the areas it has been chosen to use a grid of five by five meters. As an example Figure 6.2a and 6.2b show the Google Maps image and the reconstruction in the ENVI-met Spaces tool for the Weesperstraat. The materials are displayed in different colours, with the vegetation in green. To acquire the heights of the buildings in the locations the AHN dataset has been used. The AHN is an online available dataset that stores the heights of buildings and streets in the built environment. To identify the types of trees present at the locations the Haagse Bomen App has been used, however, in many cases ENVI-met did not have the types of trees stored in their database. In case the type could not be found it was chosen to use one of the simple trees available in the Spaces tool. Furthermore, the applications stated before provided information about the materials and surfaces present in the nine locations.

Before the simulation of the micro-climates can commence, information on time, atmospheric data, and model settings has to be provided to ENVI-met. In table 6.2 the parameters are stated which are applied in every simulation. The nesting area surrounds the core model, and provides stable lateral boundary conditions for the core model, that would be absent without the use of nesting grids. However, the



(a) Aerial image of the Weesperstraat via Google Maps.



(b) Weesperstraat 3D model in the ENVI-met Spaces tool.

Figure 6.2: Weesperstraat

Parameters	Model input value
Simulated dates	26 July 2018 till 28 July 2018
Duration time	44:00:00
Wind direction	10
Measurement height air temperature & humidity	1.5 meter
Grid size	5 meters
Nesting grids	6
Roughness length	0.01
Cloud cover (cc)	0

Table 6.2: Parameters used for every simulation in ENVI-met.

nesting grids are not part of the computational space of the model. It is decided to use 6 nesting cells for every dimension in space, hereby the model boundaries are extended which improves the simulations' computational power. Afterwards, the meteorological conditions over a 44 hour period are simulated for the nine locations.

6.1.3 Biomet

In addition to the atmospheric data needed for the determination of the [PET](#), the Biomet tool is needed to calculate the [PET](#). For the calculation of [PET](#) several parameters can be adjusted. It was considered to make a different index for both men and women, as can be seen in Figure 6.3. Therefore, a the [PET](#) was calculated once for men and once for women, however, when looking at the resulting [PET](#) maps no clear difference could be seen between them. Furthermore, it was looked into taking different ages 75 and 80. In the resulting [PET](#) maps the difference in thermal perception was minimal. Therefore, it was chosen to use 75 as age to determine the [PET](#) values.

Parameter	Female	Male
Age	75	75
Weight	70	75
Length	1.68	1.75
Clo	0.90	0.90
Work metabolism	80.21	80.21

Table 6.3: Parameters used for calculating [PET](#) values for woman and men.

6.1.4 PET results

When the simulations in ENVI-met have concluded, all the information needed for the calculation of the PET values is ready and can be calculated for every location. To make a map of the PET values, these values have to be averaged to one single value for every location in order to interpolate the values in QGIS. Three ways of averaging are compared: Average, median, modus. Figure 6.3 shows the average, median and modus of the calculated PET values for the timestamps of 04.00, 14.00, 17.00 and 24.00 o'clock for all nine locations. It can be seen that the median and average follow the same tendency. The modus however has some extreme values for the Athenesingel and the Rijswijkse Landingsbaan at two o'clock in the afternoon. The PET values are calculated on a five by five meter grid for every location, where every location covers an area of about 100 square meters. It was decided to leave out the geometric mean as it gave almost the same values as the average, differencing around 0.01 from each other. The modus however has some extreme values for the Athenesingel and the Rijswijkse Landingsbaan at 14.00. For building the index map the average value as it follows the same tendency as the median.

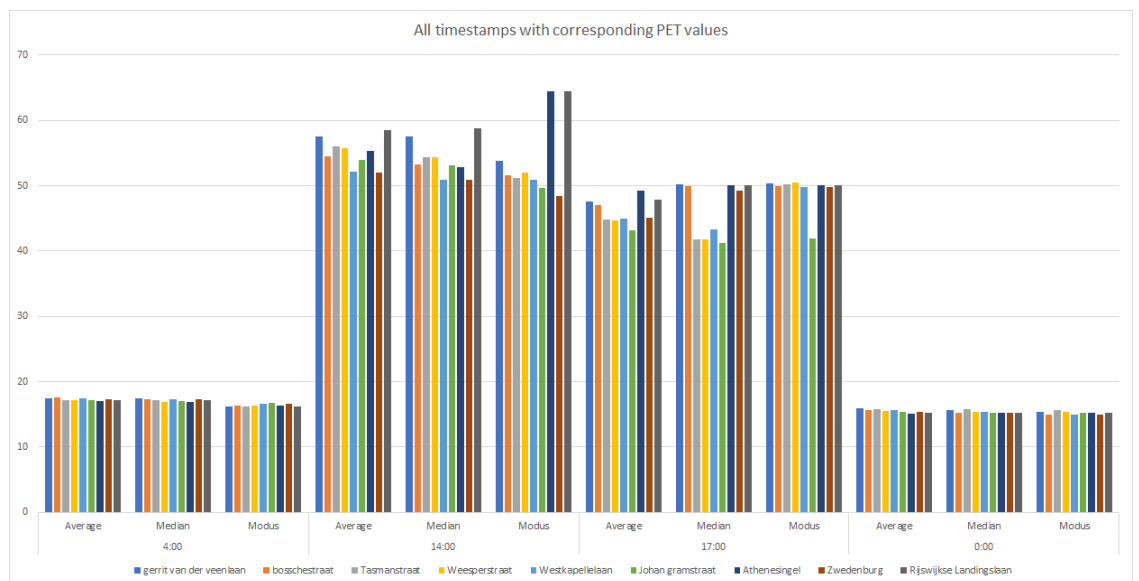


Figure 6.3: For all the timestamps the average, median and modus of the PET calculated for a man aged 75.

6.1.5 Mean radiant Temperature

The mean radiant temperature (T_{mrt}) plays a significant role in the determination of the PET. The T_{mrt} represents the human radiation load and is a parameter for micro meteorological conditions when the weather conditions are sunny [Klemm et al., 2013]. The temperatures of surfaces affect persons thermal comfort through radiant temperature. The T_{mrt} is highly explanatory for the PET as it is the most dominant factor of the way people perceive comfort [Bicol et al., 2009]. In Figure 6.4 the T_{mrt} of the Weesperstraat is displayed on 27th of July at 14.00 o'clock.

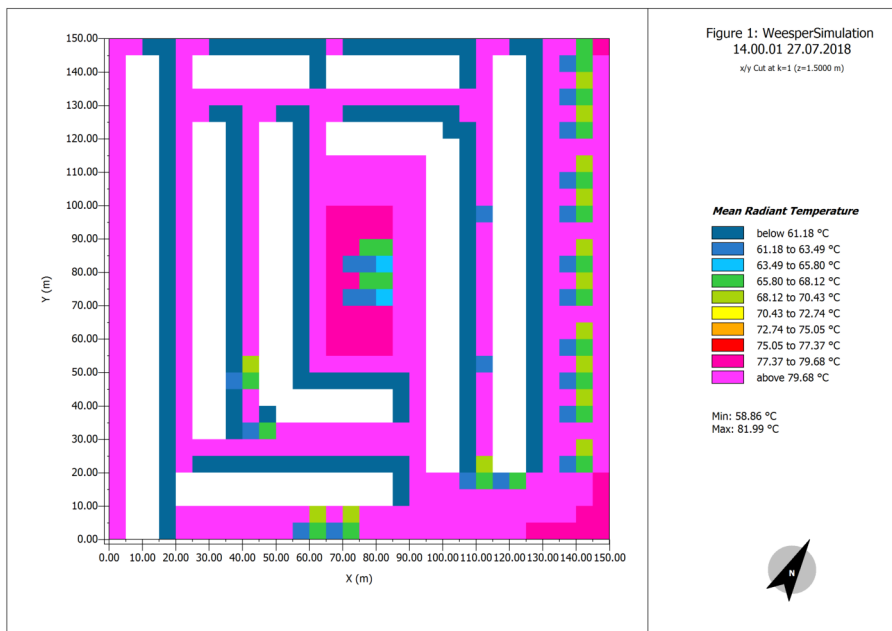


Figure 6.4: Tmrt at 14.00 o'clock in the Weesperstraat.

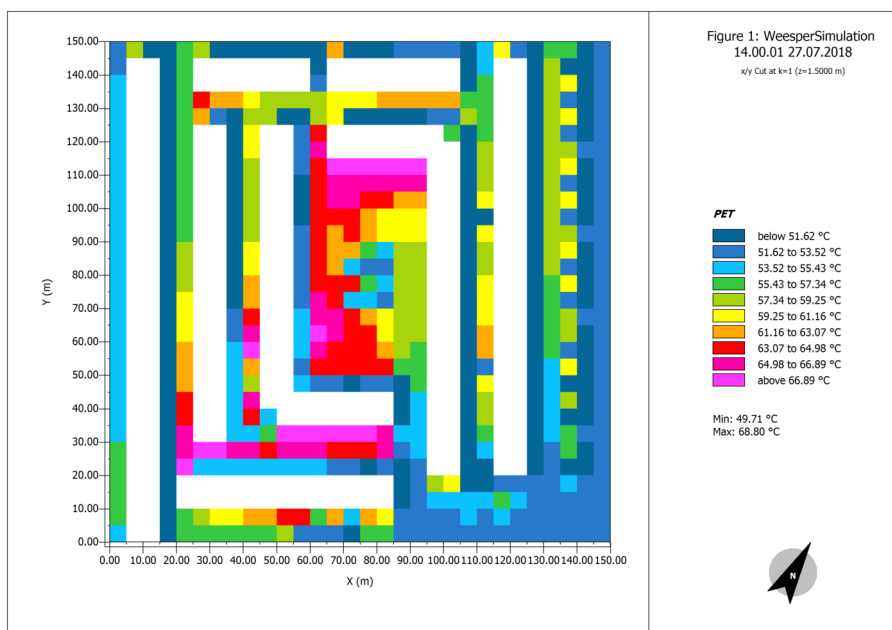


Figure 6.5: PET at 14.00 o'clock in the Weesperstraat.

6.2 HAZARD LAYER: INDOOR TEMPERATURE

Human beings spend most of their days inside and not outside. Especially the elderly, who are not very mobile any more because of old age and physical limitations spend most of their day inside their homes. Therefore, the inside temperature has been considered as being an important indicator of heat related health risk. The obtained dataset on inside temperature contains data that is aggregated on the neighbourhood level. As can be seen in Figure C.6 in the appendix the indoor temperatures are highest in the city centre. Figure C.5 in the appendix displays the amount of users having a thermometer in their homes for every neighbourhood. Especially in Leyenburg, Houtwijk, Schilderwijk-west and Nieuw-waldeck many people use the indoor thermometer (over 200 people).

6.3 EXPOSURE LAYER

The exposure layer consists of the population density of the city of the Hague and the orientation of the facade. The data needed to compose this map is retrieved from the 100m Vierkantstatistiek tiles. The map can be seen in Figure C.1. The data already fitted the 100 by 100 meter grid, and needed no further processing.

The orientation of the facade of buildings affects the thermal comfort indoor. Therefore, in this study the orientation of the street is used as an indicator of risk that is represented in the exposure layer. Keeping in mind that the sun sets in the west, the front facades having a west orientation endure the most solar radiation in the evening. Within the city of The Hague effect of the orientation of the facade on the thermal comfort inside the house is the highest when the facade is facing east or west. This means in the street is on the N, S, NW-SE, and NE-SW axis.

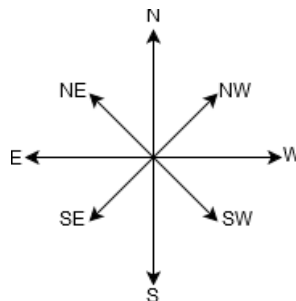


Figure 6.6: Orientations.

The streets of The Hague have a predominant road network that is orthogonally structured and orientated on NW-SE and NE-SW axis. The road network has been built parallel to the shoreline as can be seen in Figure C.3. Most buildings have their facade parallel to the road network infrastructure. To make a map of the orientation of the facades simplifications had to be made. From the spatial layer containing the buildings, only the roads with a residential function were selected as can be seen in Figure C.4. To make a subdivision in the orientation of the facades eight axes have been chosen: the north, north-east, east, south-east, south, south-west, west, and north-west axis. With manipulation in QGIS the streets of the Hague have been subdivided into the eight orientations, shown in Figure C.4. Afterwards, the eight orientations have been normalized by assigning weights to each axis. Streets following the north and south axis get the highest weight: 0.25. NE, NW, SW, SE get assigned 0.1. And the west and east axis get 0.05.

6.4 VULNERABILITY LAYER

The indicators that influence the vulnerability are: being part of the elderly population, and loneliness amongst these elderly.

The first indicator the vulnerability layer is composed of is the elderly population of the city of the Hague. The data needed to compose this map is retrieved from the 100m Vierkantstatistiek tiles. The map can be seen in Figure C.2. Further processing of this map was not necessary as it was already in the correct format. It can be seen in Figure C.2 that in the neighbourhoods in the west of the Hague and in the north the most people above the age of 75 reside.

In the original file loneliness is expressed for every neighbourhood in the Hague, as can be seen in Figure C.7. With some geo-processing steps in QGIS including joining and clipping the spatial layer has been divided into 100 meter by 100 meter tiles as shown in Figure C.8.

7

DEVELOPING THE HERI

In this chapter the weighting procedure of the spatial layers is described. To structure the decision problem and to identify the criteria and alternatives in a logical demeanour the [AHP](#) is used. In this evaluation method, with reference to previous research and considering the available free to use data the indicators that are selected are:

- [PET](#)
- Being an elderly person (75+)
- Population density
- Loneliness amongst elderly
- Indoor temperature
- Orientation of the facade

In [AHP](#) more than one decision maker is required. For this research five experts in the fields of meteorology, urbanism and environmental studies were approached and requested to decide on the relative importance between indicators in each dimension following a 1-9 fundamental scale, in which '1' indicated equal importance, and '9' presents extreme importance. The explanation of the indicators used in the questionnaire can be seen in appendix [A.1](#) and [A.2](#). It has to be noted that the indoor temperature dataset was obtained at a later moment in time then the other datasets and therefore it is not included in the questionnaire in the appendix. The expert opinions on the weight of indoor temperature were obtained by sending out an extra email in which the experts were asked to compare indoor temperature to the other indicators.

Indicators	Definition
Physiological equivalent temperature (PET)	A human bio meteorological parameter that describes the thermal perception of an individual
Age 75+	Being older than 75 years old
Orientation of the street	The orientation of the façade with respect to the sun
Indoor temperature	The temperature measured inside houses having a certain sensor installed, aggregated on the neighbourhood level
Population Density	The amount of people living per km ²
Loneliness amongst elderly	Percentage of elderly people that are lonely measured per neighbourhood

Table 7.1: Explanation of the indicators of heat vulnerability for the elderly population in the questionnaire.

7.1 AHP RESULTS

In designing the [HERI](#) for every timestamp, four [AHP](#) processes have been conducted, as can be seen in table [7.2](#). The decision to conduct four [AHP](#) processes comes from the notion that every set is composed of different indicators, and this influences the weights. The different sets are referred to in table [7.2](#). The results of the questionnaire have been put into an excel sheet developed by K. Goepel in order to calculate

the weights for the indicators through the [AHP](#) method. From each expert a judgment matrix is obtained for each dimension. Afterwards, a consistency test using a Consistency Ratio ([CR](#)) has been applied to test whether the sorting results were logically consistent.

Set-1	Set-2	Set-3
PET	PET	Indoor temperature
75+	75+	75+
Loneliness	Loneliness	Loneliness
Population density	Population density	Population density
Orientation of the facade		

Table 7.2: The three sets of indicators to make [HERI-1](#), [HERI-2](#), [HERI-3](#) and [HERI-4](#).

7.1.1 AHP result Set-1

In this section the [AHP](#) outcome is described for two indicator sets where the facade orientation is included. The [AHP](#) results can be considered as consistent when the consistency ratio is below or equal to 10%. In answering the questionnaire, two out of five experts have been consistent in answering the questionnaire. However, through combining the outcomes of the answers for Set-1 an overall consistency rate of 2.3% is obtained. The consensus amongst the expert is 78.3%, which is also sufficiently high. The final weight for the indicators in each set have been obtained by taking the geometric mean of the the outcomes of the expert opinions. The consolidation matrix of Set-1 is shown in Figure 7.1 with on the right side the importance of each of the indicators expressed in a percentage. The table shown in Figure 7.3 displays the weights of the indicators with their absolute errors. The weights of Set-1 show that the [PET](#) hazard is seen as the biggest risk for the elderly. Being an elderly person is regarded as having the second most influence on experiencing risk for during an event of excessive heat.

Matrix											normalized principal Eigenvector
	PET	75+	Orientation façade	Population density	Loneliness	0	0	0	0	0	
PET	1	2 1/4	4 2/7	5 1/7	4 1/2	-	-	-	-	-	46.42%
75+	4/9	1	3 1/6	4 1/4	1 3/5	-	-	-	-	-	24.73%
Orientation façade	1/4	1/3	1	1	3/4	-	-	-	-	-	8.66%
Population density	1/5	1/4	1	1	4/7	-	-	-	-	-	7.69%
Loneliness	2/9	5/8	1 1/3	1 3/4	1	-	-	-	-	-	12.50%

Figure 7.1: The consolidation matrix of Set-1.

Indicator	Weight	Absolute error
PET	46.4%	7.0%
Elderly (75+)	27.3%	4.2%
Loneliness	12.5%	2.7%
Orientation of the facade	8.66%	0.5%
Population density	7.9%	1.0%

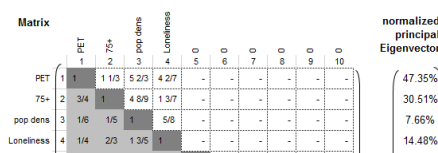
Table 7.3: Set-1 indicator weights.

7.1.2 AHP result Set-2 and Set-3

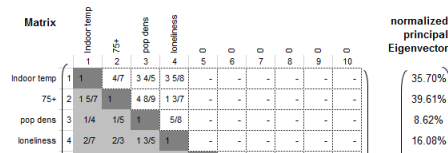
In this section the AHP outcome is described for the indicators in Set-2 and Set-3. In these sets the indicator 'orientation of the facade' has been excluded. This indicator is excluded because only for the timestamp of 14.00 the facade is influenced by the sun, making this indicator not useful for the other two timestamps.

The overall consistency ratio for Set-2 is 3.0%, which is sufficient as it is under 10%. In Figure 7.2a the consolidation matrix can be seen. The overall consensus between the decision makers is at 83.1% which indicates that the experts agree about the weights to a far extent. The weights can be seen in Figure 7.4. The PET is viewed as most important with a weight of 47.4%, followed by being 75 years or older with 30.5%. This indicates that the HERI map for this indicator set will show a great influence of the PET. Population density will almost show no influence in the HERI maps based on Set-2.

In Set-3 instead of the PET as the hazard, the indoor temperature is used. The weights can be seen in Figure 7.5. In this set the consistency ratio is 7.1% which is also under 10% and the consensus among the experts is 77.8%. Set-3 weights are more equally spread compared to the weights of Set-2. The weights for being an elderly person and indoor temperature are almost equal. The population density will have almost no influence in the HERI-3 map.



(a) The consolidation matrix of Set-2.



(b) The consolidation matrix of Set-3.

Figure 7.2: Consolidation matrices of Set-2 and Set-3.

Indicator	Weight	Absolute error
PET	47.4%	9.5%
Elderly (75+)	30.5%	7.4%
Loneliness	14.5%	4.5%
Population density	7.7%	1.2%

Table 7.4: Set-2 indicator weights.

Indicator	Weight	Absolute error
Elderly (75+)	39.6%	15.0%
Indoor temperature	35.7%	14.3%
Loneliness	16.1%	7.3%
Population density	8.6%	0.8%

Table 7.5: Set-3 indicator weights.

Table 7.6: Weights tables and their absolute errors.

7.2 COMPOSING HERI MAPS

In this section the composition of **HERI** maps based on Set-1, Set-2 and Set-3 is discussed. In creating the **HERI** maps three spatial layers are constant in every timestamp, namely: loneliness amongst elderly, population density, and being 75 years and over. These spatial layers can be seen in Figure 7.3. The **HERI** maps are given the number of the set they are based on. In order to create the **HERI** maps the five layers containing the indicators are normalized to a 0-1 scale. Afterwards, the normalized values of the spatial layers are multiplied with the weight attained through the **AHP** method. For three moments in the day an **HERI** is created: at 04.00 in the morning, 14.00 o'clock in the afternoon and 24.00 at midnight on the 27th of July 2018. The risk is split up in equal levels stated in the legend of each **HERI** map where:

- 0.01-0.20 = very low risk
- 0.20-0.30 = low risk
- 0.30-0.38 = moderate risk
- 0.39-0.50 = high risk
- 0.50-0.77 = Very high risk



Figure 7.3: Spatial layers from left to right: Loneliness amongst elderly, population density, and people above the age of 75. These spatial layers are the same in the creation of **HERI** maps for every timestamp.

7.2.1 HERI-1

The **HERI-1** map is based on Set-1 indicators, in which the facade orientation is included. Figure 7.4 displays **HERI-2** at 14.00 o'clock in the afternoon. It can be seen that the East and West of The Hague are affected the most according to this map. This can be explained by the high **PET** temperatures throughout The Hague, the indicator that received the highest weight through the **AHP** weighting method. Furthermore, the facade orientation received the second lowest weight of 8.25% and the population density only received a weight of 8.11%. It can be stated that the

influence of these indicators are negligibly small. In addition, the orientation of the facade is only measurable during daytime hours as in the night time the sun has no effect on the orientation of a house. As the heat island effect is most pronounced during night time the usefulness of this indicator is doubtful. Furthermore, the houses in newer built parts in The Hague often do not have their facades facing the streets which was checked using the web page of [Waag \[2013\]](#), where buildings are mapped together with their building age. Therefore, the Set-1 is not very suitable for the composition of a [HERI](#) map.

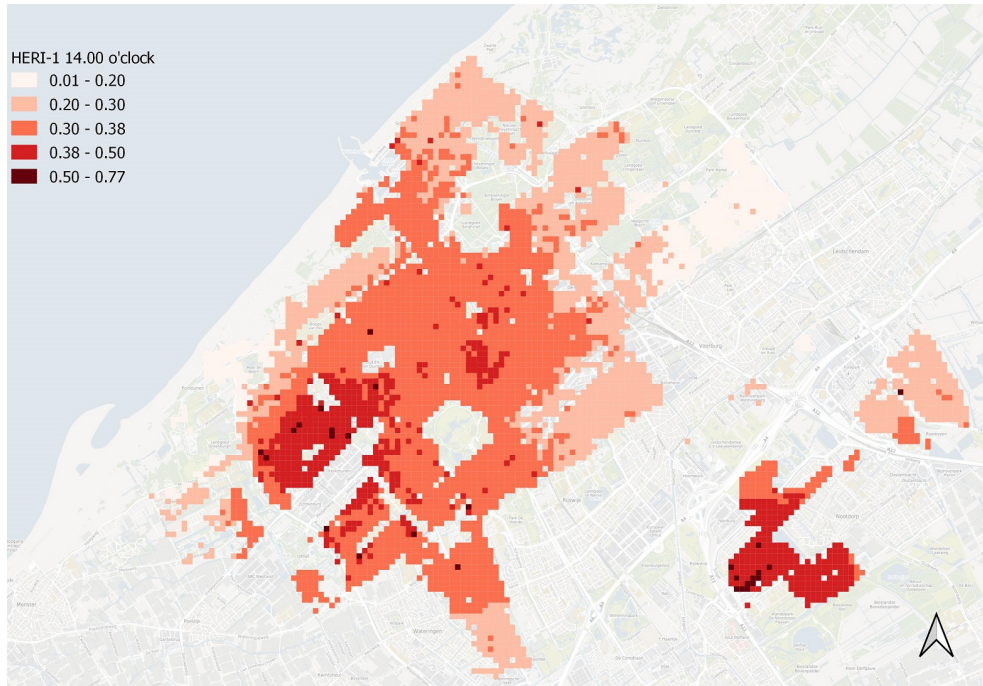


Figure 7.4: [HERI-1](#) at 14.00 o'clock in the afternoon.

7.2.2 HERI-2

Three HERI-2 maps have been designed for three timestamps on the 27th of July: 04.00, 14.00 and 24.00 o'clock. Because of the different ways of defining the average PET value for every location described in section 6.1.4, a choice had to be made between the average, the median, and the modus. It is decided that the HERI-2 maps are based on the average PET value as the median and average PET values followed the same tendency, making them very much alike. For the composition of HERI-2 the PET layer has to be adjusted for every timestamp as the values change throughout the day. The HERI-2 will be discussed for every timestamp where the PET layer is shown for explaining the results in Figure 7.5. In Figure 7.6 the HERI-2 maps for each of the three timestamps are presented.

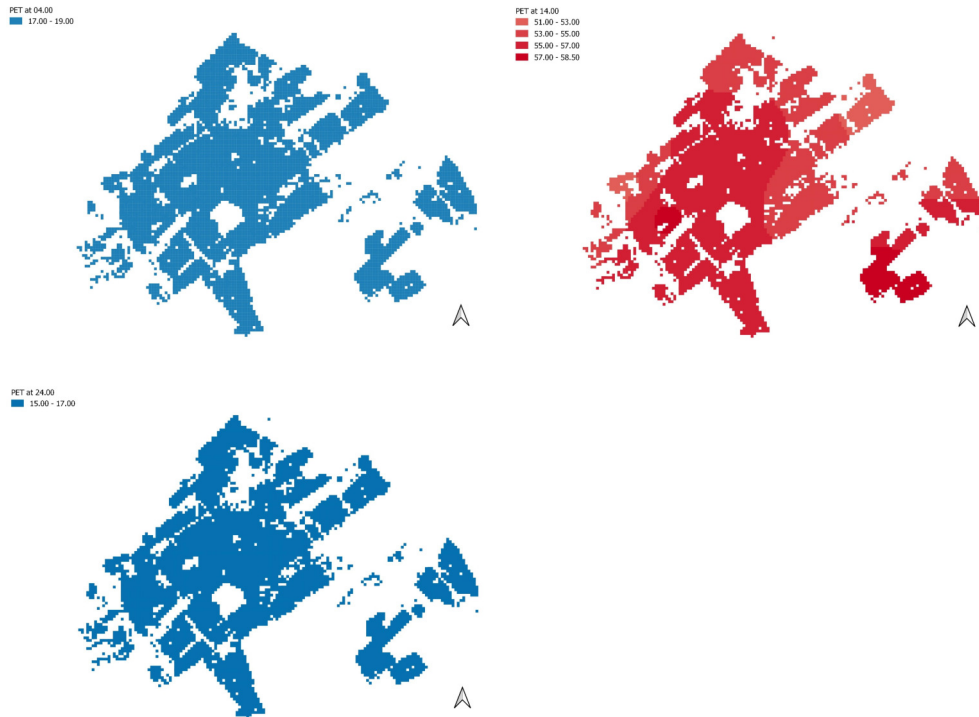


Figure 7.5: From left to right: PET temperatures for 04.00 o'clock, 14.00 o'clock, and 24.00 o'clock.

HERI-2 at 04.00 o'clock

At 04.00 o'clock in the morning the value 0.6 represents the lowest risk and 5.6 the highest risk areas for the elderly. What stands out from this index map is the north side and the west side of The Hague having high risk areas for the elderly. These high risk values range between 3.6 to 4.6. From Figure 7.3 it can be seen that the elderly live in areas depicted by the index as high risk areas. The influence of the high weight assigned to PET can be seen clearly in the high risk areas in this HERI map. Furthermore, the PET layer also causes the white spot in the low risk area in the shape of a circle in the centre of The Hague. In Figure ?? the night time is displayed where in the city centre the PET temperatures decrease to 17°C.

HERI-2 at 14.00 o'clock

After the sun comes up, the city The Hague is heating up, especially the city centre and the west. The HERI-2 of 14.00 o'clock shows a low risk of 0.72 to a high risk of 5.97. A high risk level in the central area of The Hague spreads to the borders of the municipality where the risk eventually decreases. Throughout The Hague high PET

values can be observed in Figure 7.5. The highest PET values can be seen in the east part (Ypenburg) and the west part of The Hague. The people aged 75 and older live in the west and north part of The Hague. These two layers play the biggest role in forming the HERI-2 map.

HERI-2 at 24.00 o'clock

The PET temperatures (outside) in the city centre decrease to 17°C during night time, see Figure 7.5. In the map the view is misleading as the outside temperature is only ranging around 17°C. Therefore the normalized PET values will not be representative when multiplied with its weight. Also it can be seen what the impact is of only having nine locations for calculating the PET.

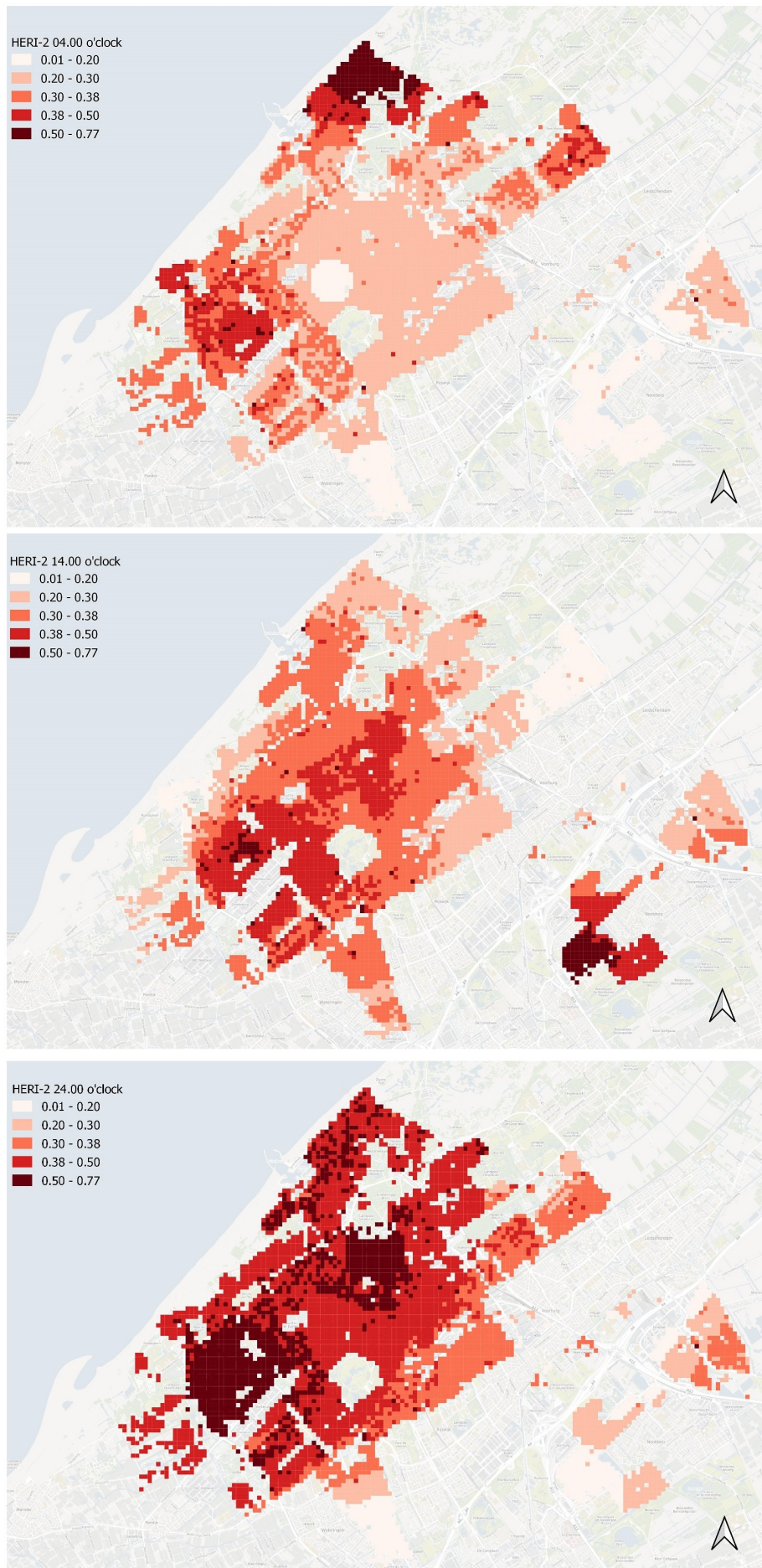


Figure 7.6: HERI-2 maps for the the three timestamps.

7.2.3 HERI-3

In this section the three HERI-3 maps have been designed for three timestamps on the 27th of July: 04.00, 14.00 and 24.00 o'clock displayed in Figure 7.8. In creating the HERI-3 three spatial layers are constant in every timestamp, namely: loneliness amongst elderly, population density, and being 75 years and over. These spatial layers can be seen in Figure 7.3. For the composition of HERI-3 the indoor temperature layer has to be adjusted for every timestamp as the values change throughout the day.



Figure 7.7: From left to right: indoor temperatures for 04.00 o'clock, 14.00 o'clock, and 24.00 o'clock.

HERI-3 at 04.00 o'clock

At 04.00 o'clock in the morning The Hague has predominantly low risk areas according to the map. What stands out from this index map is the centre of The Hague having a high risk area for the elderly. In Figure 7.7 it can be seen that in the centre the highest temperature is measured explaining the high risk area in the city centre. The other high risk areas are mostly in the grid cells where elderly live.

HERI-3 at 14.00 o'clock

At 14.00 o'clock the risk is between 0.38 and 0.50 in a big part of the Hague. It can be seen that in the areas where the indoor temperature is the highest, (see Figure 7.7), the risk is also the highest. Some parts where elderly live the risk rises to very high in the west of The Hague.

HERI-3 at 24.00 o'clock

The urban heat island effect is clearly recognizable inside the houses at night time when the temperatures indoor temperatures do not decrease as much as the PET temperatures (outside) in the city centre, see Figure 7.7. It can be seen that throughout the biggest part of The Hague the temperatures inside the homes are still between 28 to 30°C. The highest risk areas are in the city centre according to the HERI-3 map.

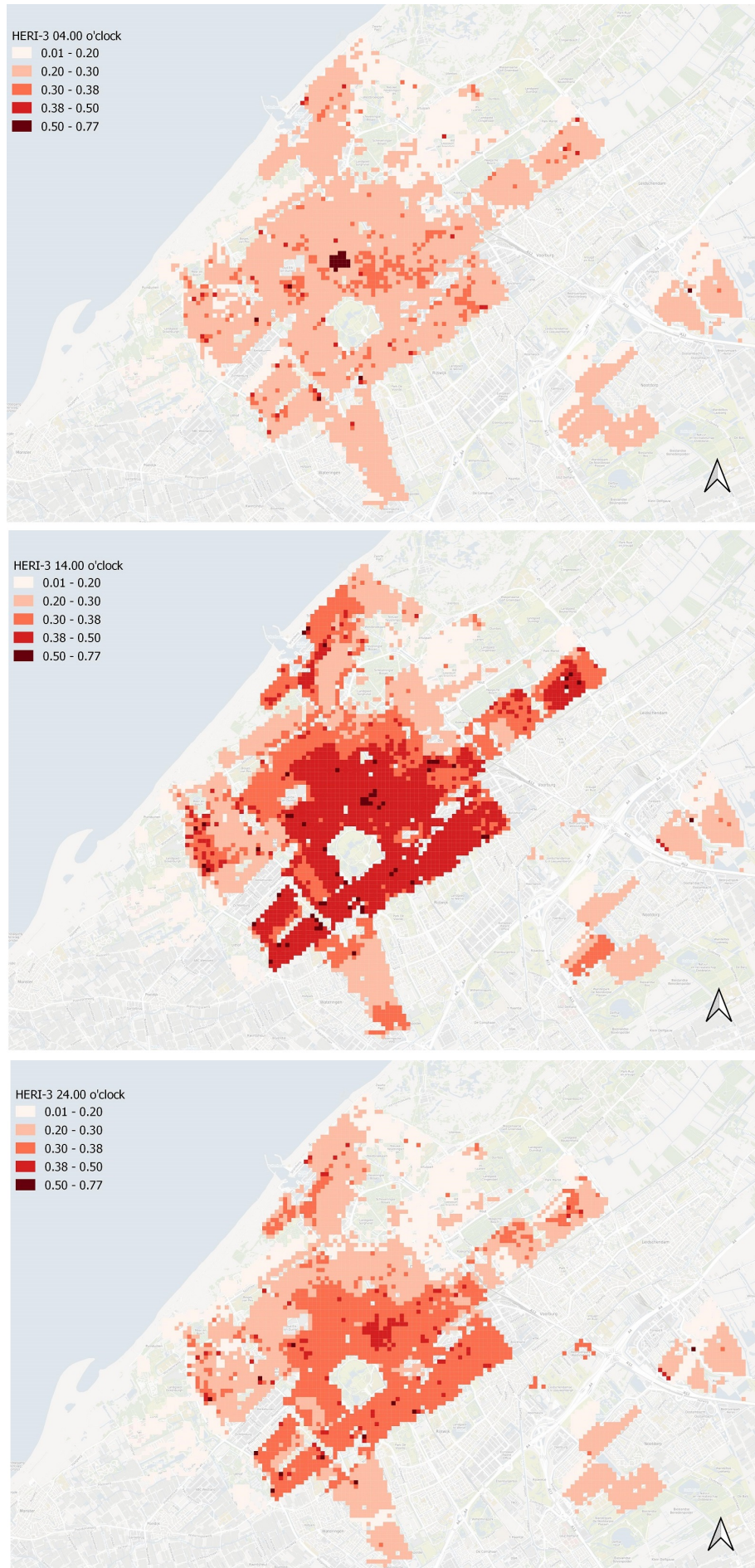


Figure 7.8: HERI-3 maps for the the three timestamps.

Conclusion HERI maps

Through composing the HERI-1 map it became clear that the facade orientation matters only throughout the day, as the sun does not shine during night time during which the facade orientation has no impact on the risk. Set-1 turned out to be not as well performing due to the weighting of the spatial layers making the influence of the facade orientation and population density negligibly small in the HERI-1 map. Therefore, Set-1 is not useful in modelling the risks elderly people are exposed to during extreme heat events. It is therefore decided on looking deeper into indicator Set-2 discussed in the next section. From the HERI-2 and HERI-3 maps a clear distinction between daytime and night time is visible. During the day both indoor temperature and PET values are high throughout The Hague. It can be seen from the night time HERI-3 that in the evening when the city cools down, inside the homes it is hard to get rid of the warmth. Especially in the city centre the risk is high for the elderly. Loneliness and population density don't play a big role in the composition of both the HERI-2 and HERI-3 maps, as their assigned weights are both under 10%. Therefore it could be decided to leave them out of the HERI maps. It is also clear that being an elderly person, PET temperature and indoor temperature have the biggest influence in the HERI maps.

7.3 VALIDATION OF THE HERI

In this section the created HERI maps are discussed and validated against a dataset on mortality among people aged 75 and older in the city of The Hague. The dataset contains the mortality of people aged 75 and older aggregated on a grid of 100 by 100 meter tiles as can be seen in 7.9. The mortality numbers after the heat wave of July 2018 will be used to perform the test of validity. By applying the bivariate Pearson Correlation a sample correlation coefficient is produced that indicates the direction and strength of linear relationships between pairs of continuous variables. With this statistical analysis the spatial layers the significance of the indicators and the HERI can be calculated. However, it is hard to establish a correlation when only one day of mortality is taken as the mortality number is too low. Therefore, the total number of people that died in the four days after the heat wave are used as to validate the HERI maps. First the correlation between mortality numbers and the separate indicators is discussed, afterwards the correlation between the HERI and the mortality is discussed.

7.3.1 Bivariate Pearson Correlation

The question is whether the mortality number amongst the elderly rises when the risk of the area increases. First, the HERI-2 maps are tested for correlation with mortality which can be seen in Figure 7.10. Here it is shown that only being an elderly person has a significant correlation to mortality where the correlation coefficient is 0.159 which indicated a weak positive correlation. The other indicators are not correlated to mortality. In Figure 7.11 a Pearson Correlation is performed with the HERI-2 maps and mortality. It can be seen that the correlation is significant. However, the positive correlation is very weak. In addition, it can be said that the indicators separately do not say anything about mortality but when put together in an index there is minor correlation.

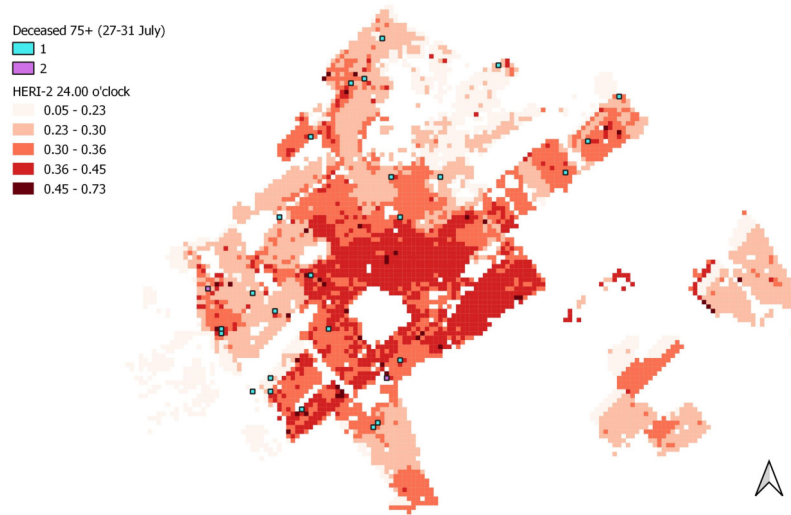


Figure 7.9: Number of deceased people of 75 or over between July 27th to July 31st 2018, together with the HERI-3 at 24.00 o'clock.

		Mortality	Population density	Being elderly (75+)	Loneliness amongst elderly	pet 04.00 o'clock	pet 14.00 o'clock	pet 24.00 o'clock
Mortality	Pearson Correlation	1	0.025	.159**	-0.001	.028*	0.000	0.023
	Sig. (2-tailed)		0.057	0.000	0.951	0.035	0.970	0.077
	N	5708	5708	5708	5708	5708	5708	5708

** . Correlation is significant at the 0.01 level (2-tailed).

* . Correlation is significant at the 0.05 level (2-tailed).

Figure 7.10: The correlation values of HERI-2 indicators with mortality amongst the elderly and their significance.

		Mortality	HERI-2 at 04.00	HERI-2 at 14.00	HERI-2 at 24.00
Mortality	Pearson Correlation	1	.073**	.060**	.064**
	Sig. (2-tailed)		0.000	0.000	0.000
	N	5708	5708	5450	5708

** . Correlation is significant at the 0.01 level (2-tailed).

Figure 7.11: The correlation values of HERI-2 maps with mortality amongst the elderly and their significance.

In Figure 7.12 the Pearson Correlation using the mortality dataset and the HERI-3 maps is shown. Comparable to the HERI-2 validation only the being elderly (75+) indicator is significantly correlated to mortality. When looking at the Pearson correlation of the HERI-3 maps with mortality HERI-3 at 04.00 o'clock in the morning explains the mortality the most. However, this link is very weak and therefore it is hard to say whether it explains it at all.

		Mortality	Population density	Being elderly (75+)	loneliness amongst elderly	indoor temperature 04.00	indoor temperature 14.00	indoor temperature 24.00
Mortality	Pearson Correlation	1	0.025	.159**	-0.001	0.000	0.006	-0.004
	Sig. (2-tailed)		0.057	0.000	0.951	0.985	0.634	0.789
	N	5708	5708	5708	5708	5539	5562	5562

** . Correlation is significant at the 0.01 level (2-tailed).

* . Correlation is significant at the 0.05 level (2-tailed).

Figure 7.12: Correlation of indicators with mortality used to create HERI-3.

		Mortality	HERI-3 at 04.00	HERI-3 at 14.00	HERI-3 at 24.00
Mortality	Pearson Correlation	1	.106**	.078**	.089**
	Sig. (2-tailed)		0.000	0.000	0.000
	N	5708	5539	5348	5562

** . Correlation is significant at the 0.01 level (2-tailed).

Figure 7.13: The correlation values of HERI-2 maps with mortality amongst the elderly and their significance.

7.3.2 Conclusion validation

The validation results show that the indicators separately are not associated with mortality except for being and elderly person (75+). However, the HERI maps show that when the weighted indicators are combined into an index a very weak correlation with mortality can be detected. It is nonetheless not evident that the HERI maps are the correct way to model the risks of urban heat islands for the ageing society. Furthermore, it would be valuable to research other statistical analysis methods for validation.

8

CONCLUSIONS

The objective of this project is to study the integration of spatial and socio-demographic data to produce a heat index for the elderly population of The Hague. This chapter summarises the findings of the conducted study by answering the research questions. Furthermore this section provides conclusions and a discussion of the results and ends with suggestions for future research.

8.1 RESEARCH QUESTIONS

What are the indicators that influence the heat related health risks the elderly population is being exposed to?

Through literature research in combination with available datasets the selected indicators were determined. The [PET](#), indoor temperature, facade orientation, population density, loneliness amongst elderly, and being 75 years or older.

- The [PET](#) gives information about the way the elderly experience thermal comfort outside.
- The indoor temperature shows what temperatures people experience during heat waves inside their homes.
- The orientation of the facade can show the relation between outdoor and indoor. The orientation affects the solar gain inside the building and thereby affect the indoor temperature.
- The loneliness amongst the elderly show on the neighbourhood level where the elderly are feeling the most lonely. The elderly are especially at risk because of the potential decrease in social contacts which leads to increased vulnerability and eventually can end in death.
- The population density shows how many people live in an area can be used to check whether the amount of people affect the risk elderly experience during heat events.

It became clear that the facade orientation and the indoor temperature could not be placed in the same index, and therefore, two sets of indicators were used to create different [HERI](#) maps. It was decided that the indicator set containing the facade orientation did not meet the requirements to make a [HERI](#) map. The indicator set including the indoor temperature was chosen to make the [HERI](#) maps for the three timestamps.

What framework is most applicable for analysing the urban heat related risks for the elderly?

In this thesis a method is developed in which different datasets and methods are combined in order to form [HERI](#) maps. It was decided to use the framework applied by [Morabito et al. \[2015\]](#) which uses the Crichton's triangle of risk as a starting point. In this risk assessment theory the triangle exists out of three components: the hazard, the exposure and the vulnerability, which have to be spatially coincident in

order for risk to exist. It is important to note that the indicators chosen to represent the hazard, exposure and vulnerability do not explain each other. The [PET](#) and the indoor temperature represented the hazard in this study. For the exposure layer the population density, and the facade orientation have been chosen. As vulnerability layer the people aged 75 or over and the loneliness amongst elderly were determined. Thereafter it was chosen to use the [AHP](#) to assign weights to the indicator layers in order to combine them. This weighting method turned out to be suitable for this research, as it was recommended by other researchers for weighting spatial layers.

Where in The Hague are the elderly population affected the most by urban heat islands?

The [HERI](#) maps have shown that during the day different places in The Hague are affected by the urban heat island effect when using the indicators determined in this thesis. From the [HERI-2](#) maps the west and the north of The Hague turned out to have the highest risk areas. According to the [HERI-3](#) maps a small part of the west, and the city centre Hague are affected the most by the urban heat island from the perspective of an elderly person. During night time it became clear that within the homes the temperatures decreased very slowly, especially in the west and centre part of The Hague.

What spatial resolution is most appropriate to visualize the urban heat related risks for the elderly population?

When visualizing the heat related risks for the elderly population datasets of different formats had to be manipulated in order to combine them into a [HERI](#) map. Due to privacy issues that come with using data about people the appropriate resolution came down to a 100 meter by 100 meter grid structure. In this resolution the data can not be used to trace the addresses of people. Furthermore, this grid size turned out to give a detailed enough display of the heat related risks for the elderly.

8.2 CONTRIBUTION AND REFLECTION

This graduation thesis started in September 2018, in cooperation with the TU Delft. Right from the start the topic of this thesis has been actual as heat waves are events that are increasing in frequency. This is an issue for cities in the Netherlands and and all around the world.

Geomatics is an applied science that deals with the modelling, acquisition, analysis, visualization, and management of geographic information with the goal of a better understanding of the built and natural environment, and solving problems in the real world. In this study multiple datasets have been combined: both social demographic datasets and spatial datasets have been put together. In bringing these datasets together new geospatial information has been created. Furthermore, location plays an important role in this research. The different indicators are all of different importance depending on location within The Hague. Based on the location and importance of the information in the spatial layers the index could be composed.

In doing research the process is never linear, which I discovered hands on during the making of this thesis. In order to develop the method many choices had to be made and this has not always been easy as time was limited and many options had to be explored. I chose to base the decisions mostly on literature. I had to combine different datasets and had to figure out how to do this in a reasonable manner. A

big help in using the datasets has been [QGIS](#) and the infinite amount of information about this software on the internet.

Throughout the course of this thesis I learned how to use ENVI-met, improved my SQL coding for data manipulation in PostgreSQL, and improved my skills in QGIS. Furthermore, I improved my soft skills as well by approaching experts. Thereby I learned how to transmit my findings to an audience in a understandable way through giving the presentations at the P2, P4 and the upcoming P5.

In the beginning of the thesis the plan was to use Netatmo sensors for the determination of the [PET](#) throughout The Hague. However, ENVI-met, the software which determines the [PET](#), is developed for using weather measurements from weather stations outside of the city. Therefore, I had to change my methodology which prolonged my thesis.

8.3 FUTURE WORK AND RECOMMENDATIONS

Multiple future research opportunities can be identified in this project. As a result of time limitations, not all aspects of creating an index have been researched or worked out. Therefore, this section provides an overview of proposed future research.

In future research it would be valuable to develop a more inclusive index, in which also women are to be considered. It has to be researched whether it would make a difference when a distinction is made between genders. This can be done by creating a separate index for women in the age of 75. Also a distinction could be made in age, where different age categories could be put into an index in order to make more precise representations. In this research the elderly population has been used as vulnerable part of the society. The other extreme age group that is affected by heat are children in the age of zero to five years old.

It would be highly interesting to use extra datasets on illness amongst elderly people. In other countries such as the UK this data is already available for usage in the making of vulnerability indexes, for example Tomlinson et al. [2011] uses data on people with ill health in composing their index. Furthermore, datasets on NDVI or land surface temperature could also be included in the process of making the [HERI](#) a more accurate representation of the risk the elderly experience during extreme heat events.

To make the index more visually attractive and understandable a dynamic viewer could be developed. This could make it possible to look through different timestamps in a day but also during the length of a heat wave. In addition, making multiple [HERI](#) maps for each day in a heat wave would greatly improve the understanding of the risks for the elderly throughout a heat wave. This can help planners and designers in their process of building a more heat resilient city.

To calculate the [PET](#) ENVI-met has been used which is heavy and costly software. In order to make the process of creating a [HERI](#) less costly other software should be looked into. In the case of ENVI-met software such as Rayman Pro (freely accessible), can be used for calculating the [PET](#). Another benefit is that Rayman Pro does not require a license. It would be valuable when it is researched whether Rayman meets the standard of ENVI-met.

The developed method in this thesis covers all the steps needed to get from the collection of relevant datasets to constructing a heat risk index focussed on the elderly society in the city of The Hague. As a result, a heat risk index is developed for the elderly to improve the current data representation and support dynamic decision-making processes. However some parts in this research have not been thoroughly described or examined. It is therefore important to point out points of criticism.

Firstly, the index has been based on spatial layers which each have information that is aggregated on different levels. Some spatial layers contain information on a 100 meter by 100 meter grid level and other on the neighbourhood level. All the layers have been converted in a 100 meter by 100 meter grid. The spatial resolution of these layers is not being taken into account when combining them together. The result of this can be seen in the resulting index maps where large patches appear in the index as a result of the neighbourhood level aggregated maps.

Furthermore, due to time limitations, only three moments during the hottest day of the summer of 2018 have been selected for the development of the [HERI](#) maps. However, as a result of this limitation only an index of one day is created. It would have been a more complete representation of the risks if more days during the heat wave had been taken into account. In the developed framework it is possible to adjust the maps for other days during the heatwave, however, this is a time consuming process and has to be improved in order to be useful.

Another point of discussion is the [PET](#) layer. For composing this layer nine locations were chosen in The Hague. The influence of using nine locations was very clear in the resulting [PET](#) layer as the influence of the interpolation influenced the appearance of the map greatly as large parts of the Hague are influenced by one [PET](#) value. It can be argued that the usefulness of this map is determined by the amount of locations for which the [PET](#) is calculated.

In creating the index many different choices had to be made. The [AHP](#) method for establishing the weights of the indicators has not been checked against other weighting procedures. This could yield a different more accurate way of weighting the indicators. Furthermore, the indicators each have been assigned a certain weighted and were used like this for every time stamp. However, for each moment in the day indicators can have different weights as the [PET](#) and indoor temperature differ throughout the day. In the normalization procedure of the spatial layers it

In determining the [PET](#) values ENVI-met software has been used. This is very heavy and costly software. In order to make the developed method cheaper and more accessible free open software could be used as well such as Raymann Pro. Furthermore, the [PET](#) layer now is based on men of 75 years old and thereby excludes half of the society. This decision was made because of time limitations, however, in this time and age research calls for a more inclusive approach.

As validation the Pearson Correlation is applied to the resulting [HERI](#) maps. In this method the dependent variable is expected to be continuous which means it

is measured on a interval or ratio scale. However it can occur that the dependent variable is nominal with only few categories which means that linear regression is not an option. The technique that is most similar to linear regression is logistic regression analyses. This technique is of use when the dependent variable is of dichotomous nature: only two categories exist. With the mortality dataset it can be stated that there are two states the elderly person can be in: Death or alive. It can be argued that for this research the validation part other statistical methods, such as logistic regression, had be tried to find out to what extent the [HERI](#) maps can say something about the risk for elderly in case of extreme heat events.

Questionnaire

In this study high-resolution heat-related risk index maps of the city of The Hague are developed, with a focus to the elderly population (people aged 65 or over) during the heat wave of 2018. The goal is to provide more insight into the factors contributing to, and the consequences of the UHI phenomenon for the elderly population. In this study, the risk concept is represented by harmful health consequences for elderly people resulting from the interaction between three components that together form a triangle: natural hazard, exposure, and vulnerability, see figure 1. The risk is defined as a function of these three components. There is no risk if any component of the triangle is zero.



Figure 1: Risk triangle

The *hazard* is represented by the Physiological Equivalent Temperature (PET). *Exposure* to the natural hazard is depicted by the total population census data. The *vulnerability* is represented by the elderly population (over 65), the orientation of the facade with respect to the sun, and the loneliness among the elderly measured in every neighborhood. The final risk index map is generated from the spatial interaction of all of the components into a composite map. In this questionnaire the factors contributing to the heat related health risk are being compared with each other. In table 1 the indicators are explained.

Indicators	Definition
Physiological equivalent temperature (PET)	A human bio meteorological parameter that describes the thermal perception of an individual
Age 65+	Being older than 65 years old
Orientation of the street	The orientation of the façade with respect to the sun
Population density	The amount of people living per km ²
Loneliness	Percentage of elderly people that are lonely measured per neighborhood

Table 1: Explanation indicators

Figure A.1

Compare the relative IMPACT with respect to: Vulnerability to heat for the elderly (65+).
Please assign the color red to the chosen number.

1=equal 3=moderate 5=strong 7=very strong 9=extreme

1	PET	9	8	7	6	5	4	3	2	1	2	3	4	5	6	7	8	9	Loneliness
2	Age 65+	9	8	7	6	5	4	3	2	1	2	3	4	5	6	7	8	9	PET
3	Orientation of the façade	9	8	7	6	5	4	3	2	1	2	3	4	5	6	7	8	9	Age 65+
4	Population density	9	8	7	6	5	4	3	2	1	2	3	4	5	6	7	8	9	Orientation of the façade
5	Loneliness	9	8	7	6	5	4	3	2	1	2	3	4	5	6	7	8	9	Population density
1	PET	9	8	7	6	5	4	3	2	1	2	3	4	5	6	7	8	9	Population density
2	Age 65+	9	8	7	6	5	4	3	2	1	2	3	4	5	6	7	8	9	Loneliness
3	Low income	9	8	7	6	5	4	3	2	1	2	3	4	5	6	7	8	9	PET
4	Orientation of the façade	9	8	7	6	5	4	3	2	1	2	3	4	5	6	7	8	9	Age 65+
5	Loneliness	9	8	7	6	5	4	3	2	1	2	3	4	5	6	7	8	9	Orientation of the façade
1	PET	9	8	7	6	5	4	3	2	1	2	3	4	5	6	7	8	9	Orientation of the façade
2	Age 65+	9	8	7	6	5	4	3	2	1	2	3	4	5	6	7	8	9	Population density
3	Orientation of the façade	9	8	7	6	5	4	3	2	1	2	3	4	5	6	7	8	9	Loneliness
4	Population density	9	8	7	6	5	4	3	2	1	2	3	4	5	6	7	8	9	PET
5	Loneliness	9	8	7	6	5	4	3	2	1	2	3	4	5	6	7	8	9	Age 65+
1	PET	9	8	7	6	5	4	3	2	1	2	3	4	5	6	7	8	9	Age 65+
2	Age 65+	9	8	7	6	5	4	3	2	1	2	3	4	5	6	7	8	9	Orientation of the façade
3	Orientation of the façade	9	8	7	6	5	4	3	2	1	2	3	4	5	6	7	8	9	Population density
4	Population density	9	8	7	6	5	4	3	2	1	2	3	4	5	6	7	8	9	Loneliness
5	Loneliness	9	8	7	6	5	4	3	2	1	2	3	4	5	6	7	8	9	PET

Figure A.2

B

SCRIPT FOR FILLING THE DATABASE

```
import os
import datetime
import psycopg2

directory = "D:\MasterThesis\sensor_measurements"

def connect_db():
    try:
        global conn
        # creating db connection object
        conn = psycopg2.connect("host=localhost password=Taartschep.2 dbname=Rapport
user=postgres")
        global cur
        cur = conn.cursor() #used to execute commands
        print "Connected."
    except (Exception, psycopg2.DatabaseError) as error:
        print (error)

def create_table():
    cur.execute(""" Drop table IF EXISTS Rapport""")
    cur.execute("""
CREATE TABLE Rapport (
    measure_id float NOT NULL PRIMARY KEY,
    Sensor geometry,
    Date date,
    Time time,
    MAC text,
    Altitude float,
    Temperature float,
    Humidity float,
    Rain_60min float,
    Rain_24h float,
    Pressure float )
""")
    print "Table created."
    conn.commit()

def insert_to_db():
    measure_id = 0
    inserted = 0
    failed = 0
    for filename in os.listdir(directory):
        if filename.endswith(".txt"):

            with open(os.path.join(directory, filename)) as f:
                content = f.readlines()[1:]
                id = 0
                for line in content:
```

Figure B.1

```

row = line.strip().split(",")
coordinates = 'POINT(%s %s)' % (row[2], row[1])
# Specify time
time = filename.split("_")
day = datetime.datetime.strptime(time[0], '%Y-%m-%d').date()
time = datetime.datetime.strptime(time[1], '%H_%M_%S').time()
row = ['NULL' if v is "" else v for v in row]
id+=1
measure_id+= 1
strsql = "INSERT INTO Rapport (measure_id, Sensor, Date, Time, MAC, Altitude,
Temperature, Humidity, Rain_60min, Rain_24h, Pressure) VALUES({}, ST_GeomFromText('{}', {}),
'{}','{}', '{}', {}, {}, {}, {}, {});".format(measure_id, coordinates, 4326, day, time, row[0], row[3], row[4], row[5],
row[6], row[7], row[9])
try:
    cur.execute(strsql)
    conn.commit()
    inserted += 1
except psycopg2.Error as e:
    print('Insert failed: ' + str(e))
    failed += 1
    print strsql
print filename
print 'Number of rows inserted {}'.format(inserted)
print 'Number of rows failed {}'.format(failed)

if __name__ == '__main__':
    connect_db()
    create_table()
    insert_to_db()

```

Figure B.2

C

SPATIAL LAYERS

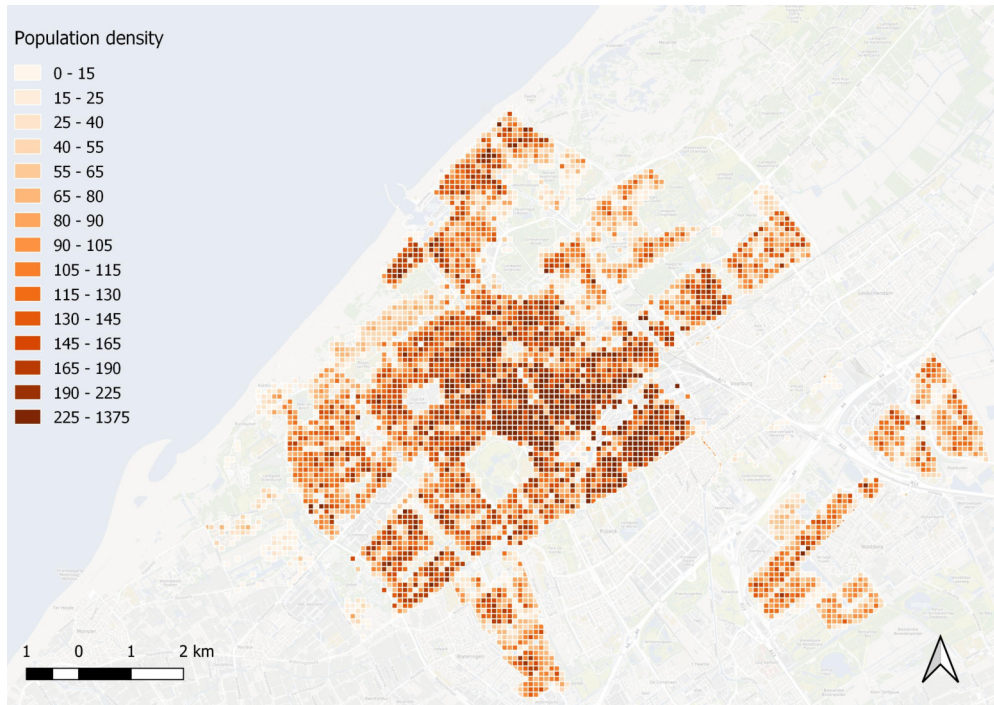


Figure C.1: Population density in the city of The Hague.

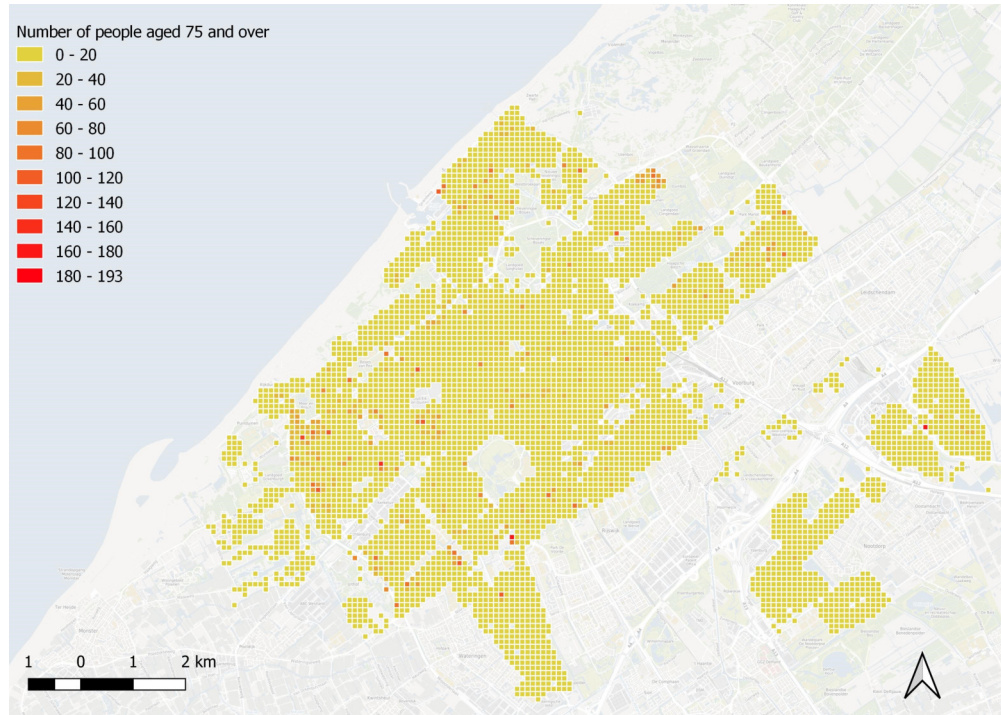


Figure C.2: Population above the age of 75 in the city of The Hague.

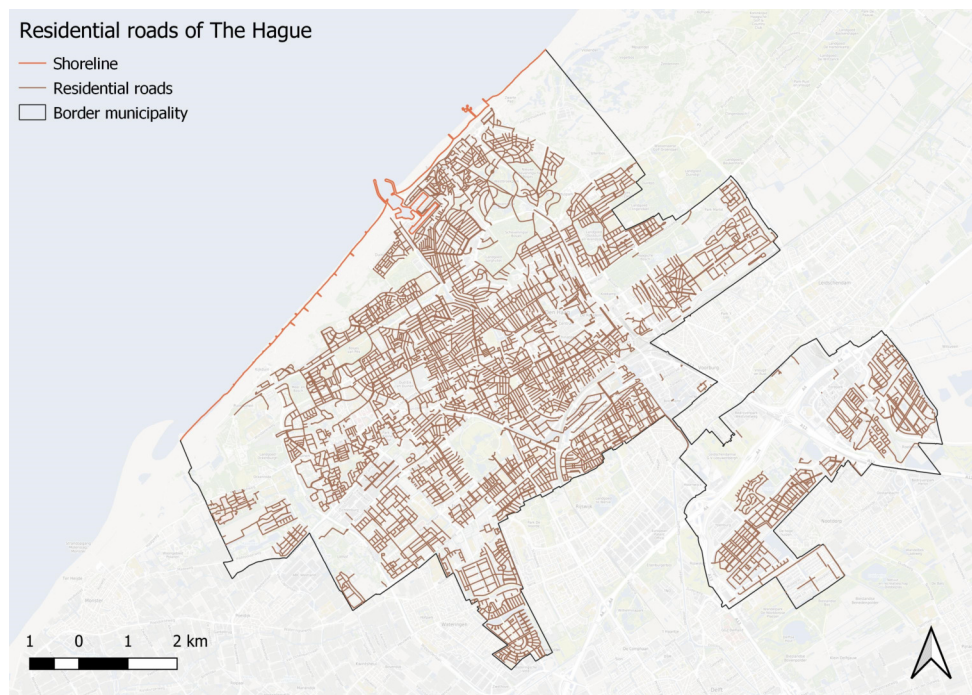


Figure C.3: Streets displaying structure of The Hague.

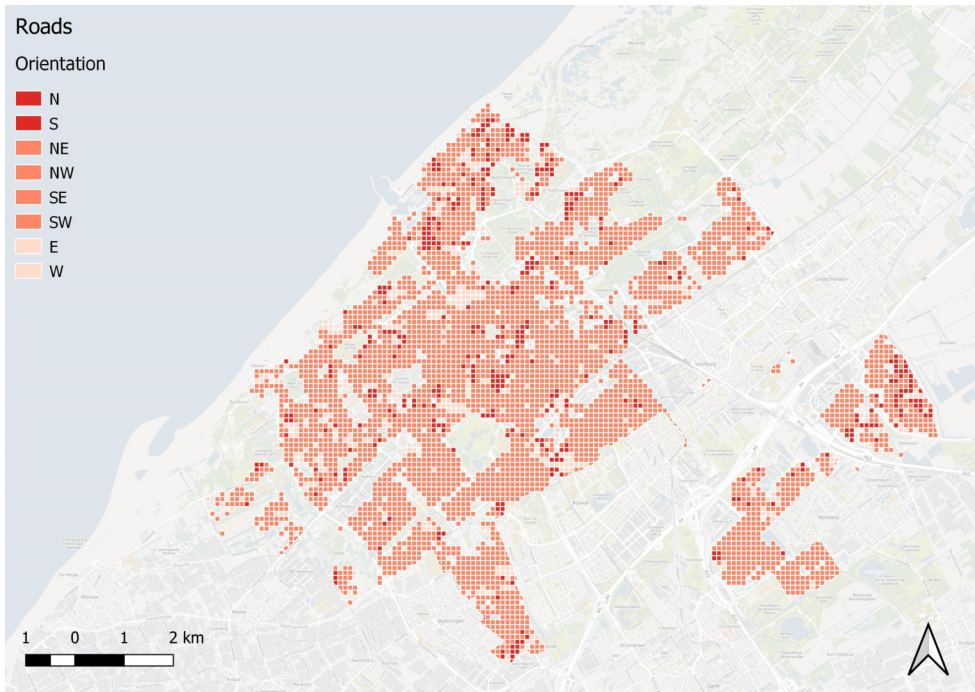


Figure C.4: Orientation of facades divided into tile structure.

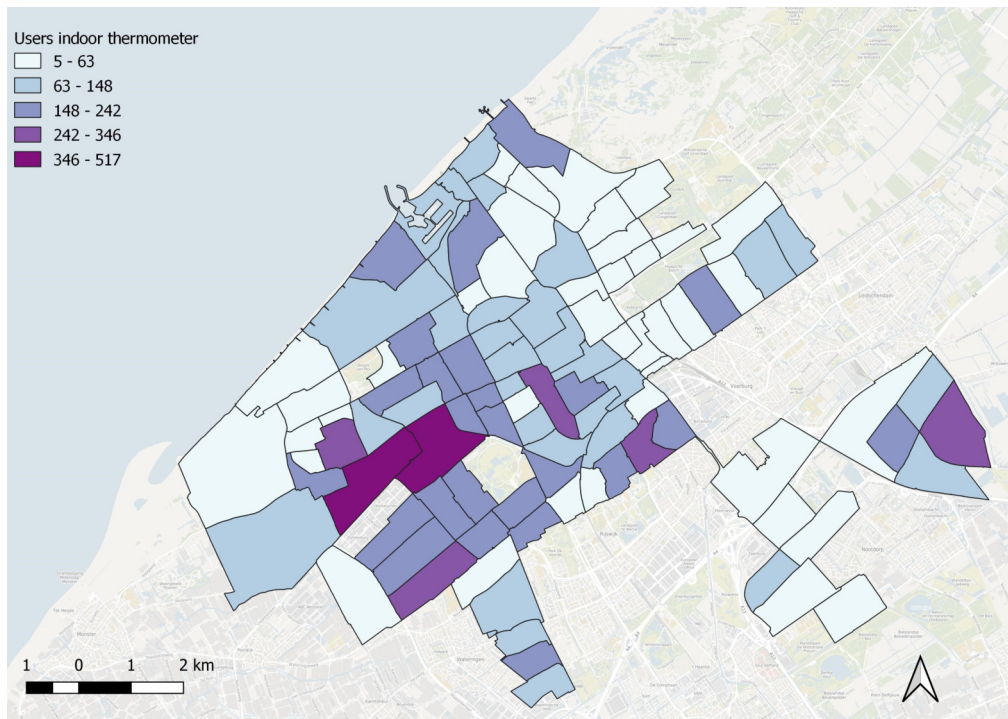


Figure C.5: The number of people using a thermometer to measure the temperature in their homes aggregated at neighbourhood level.

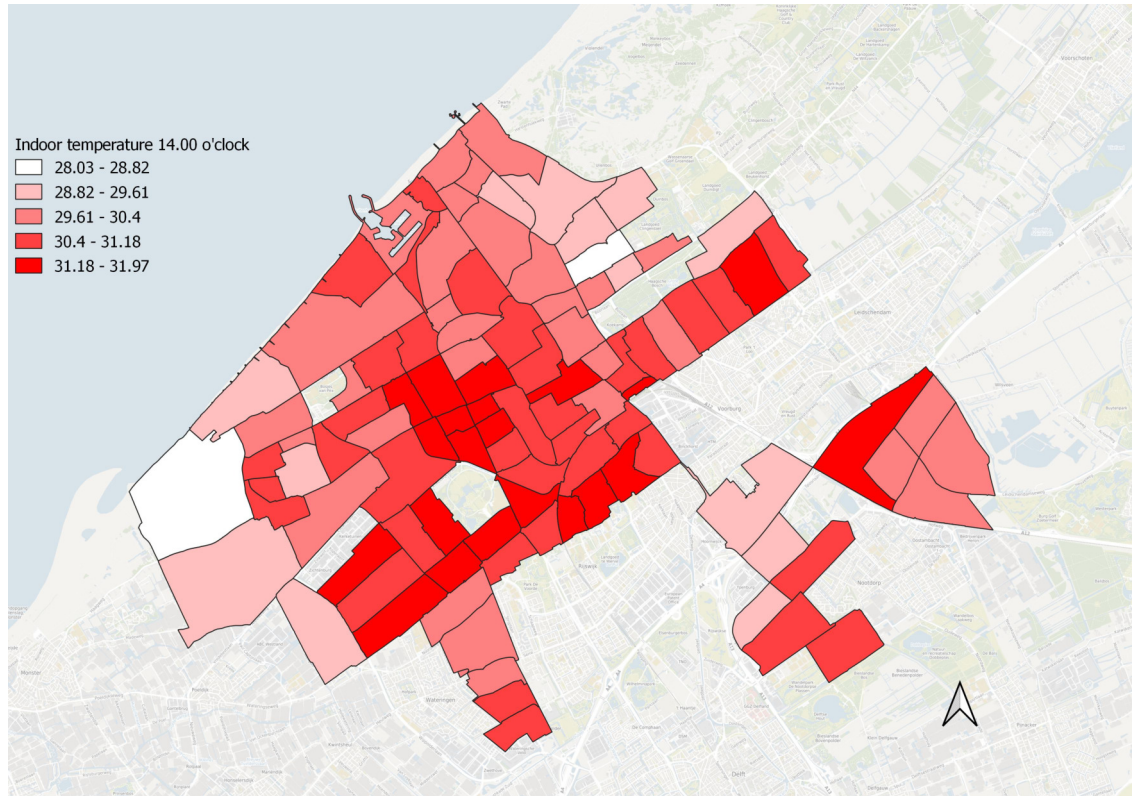


Figure C.6: Indoor temperature measured inside homes at the 27th of July at 14.00 o'clock, aggregated at neighbourhood level.

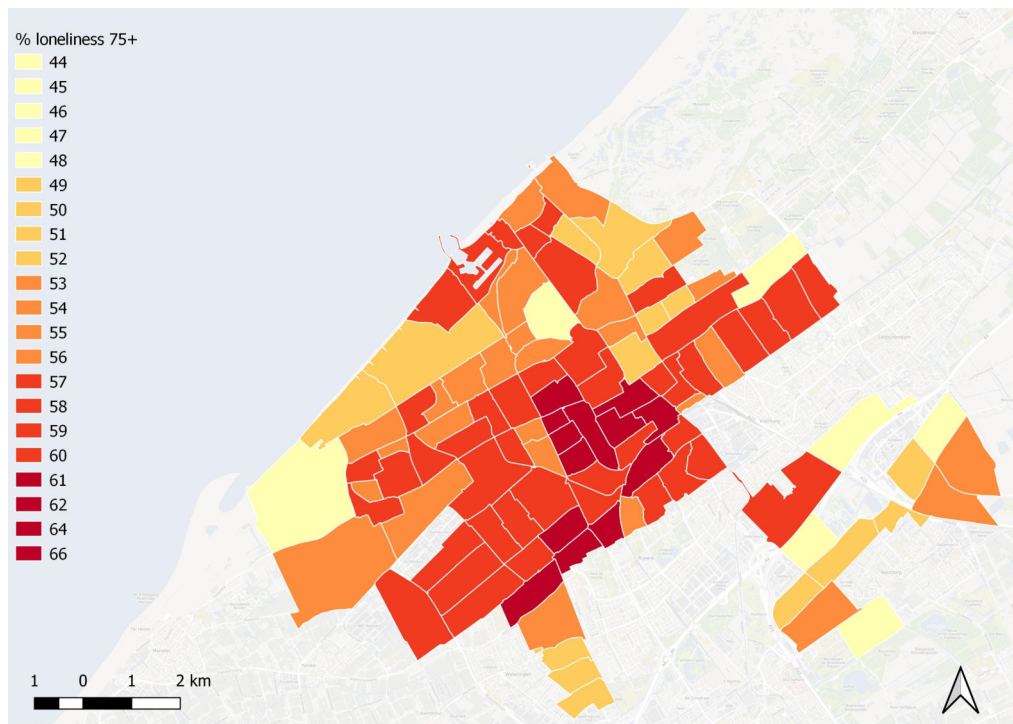


Figure C.7: Percentage of lonely elderly (75+) for every neighbourhood.

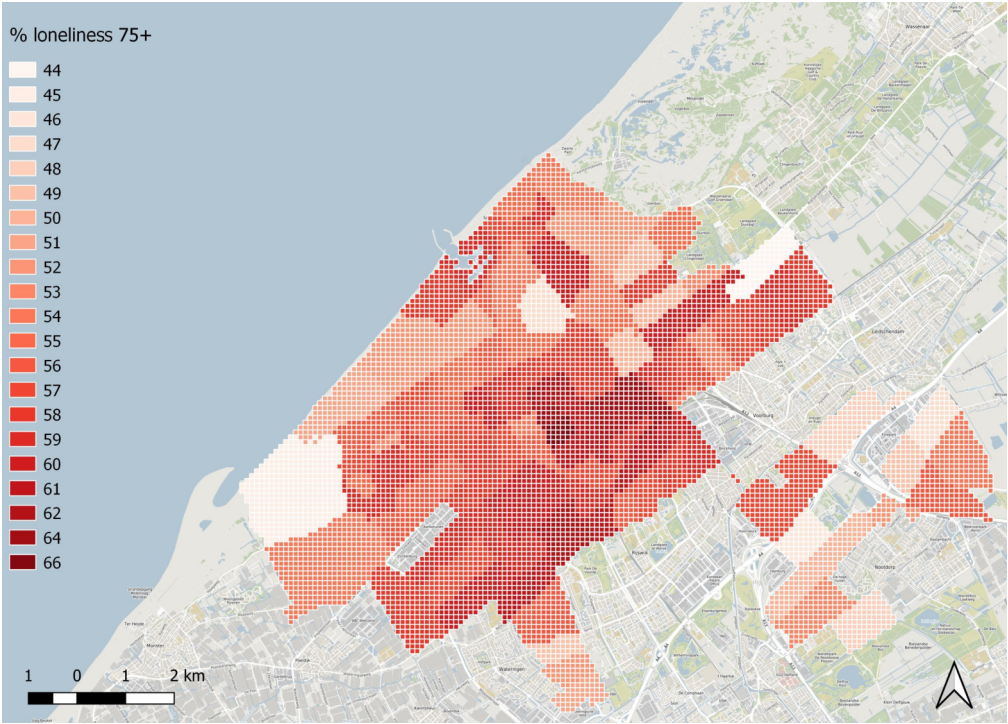


Figure C.8: Percentage of lonely elderly (75+) tiles.

D | INDEXES

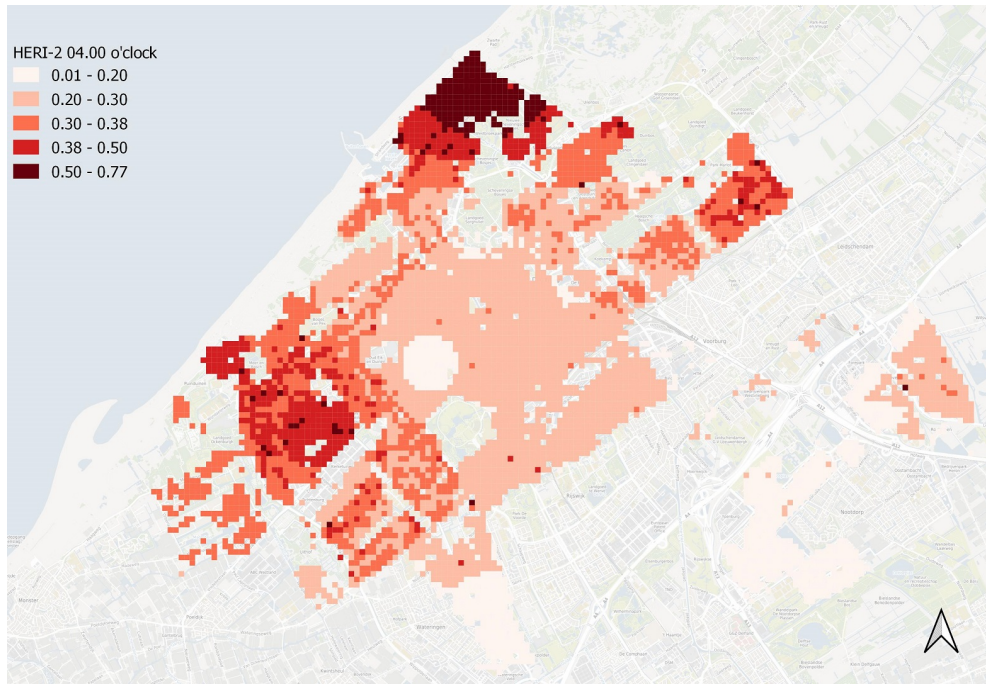


Figure D.1: HERI-2 at 04.00 o'clock in the morning at the 27th of July.

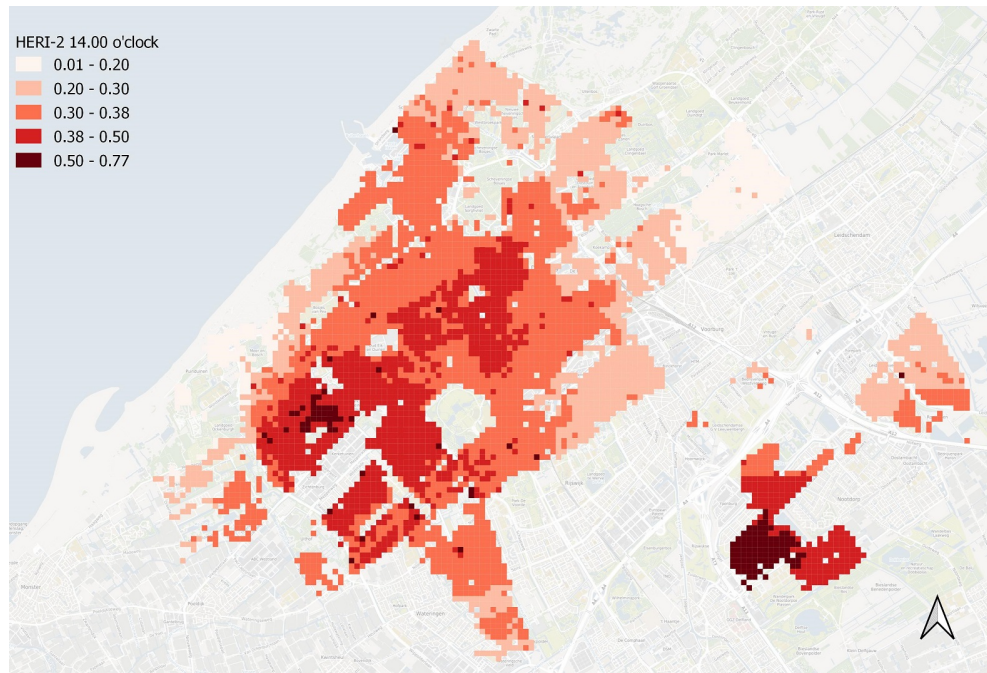


Figure D.2: HERI-2 at 14.00 o'clock in the afternoon at the 27th of July.

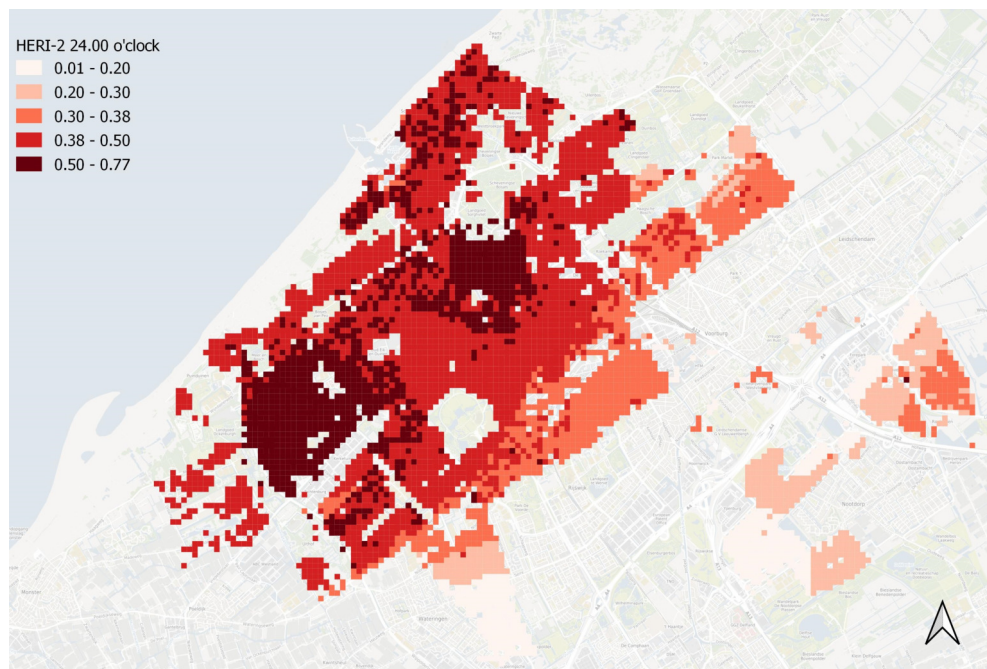


Figure D.3: HERI-2 at 24.00 o'clock at night at the 27th of July.

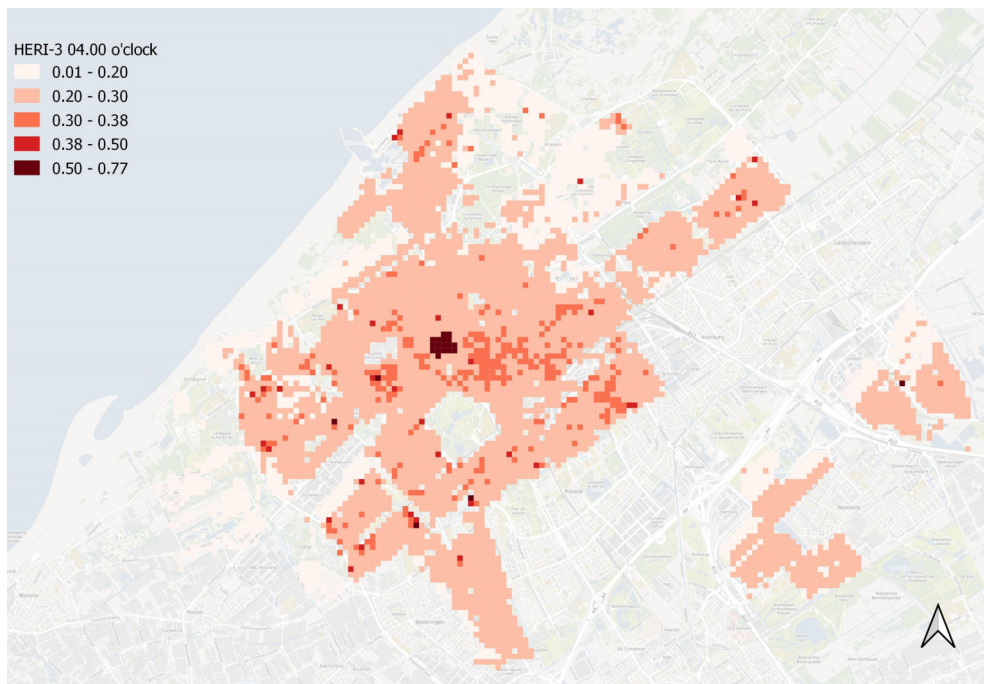


Figure D.4: [HERI-3](#) at 04.00 o'clock in the morning at the 27th of July.

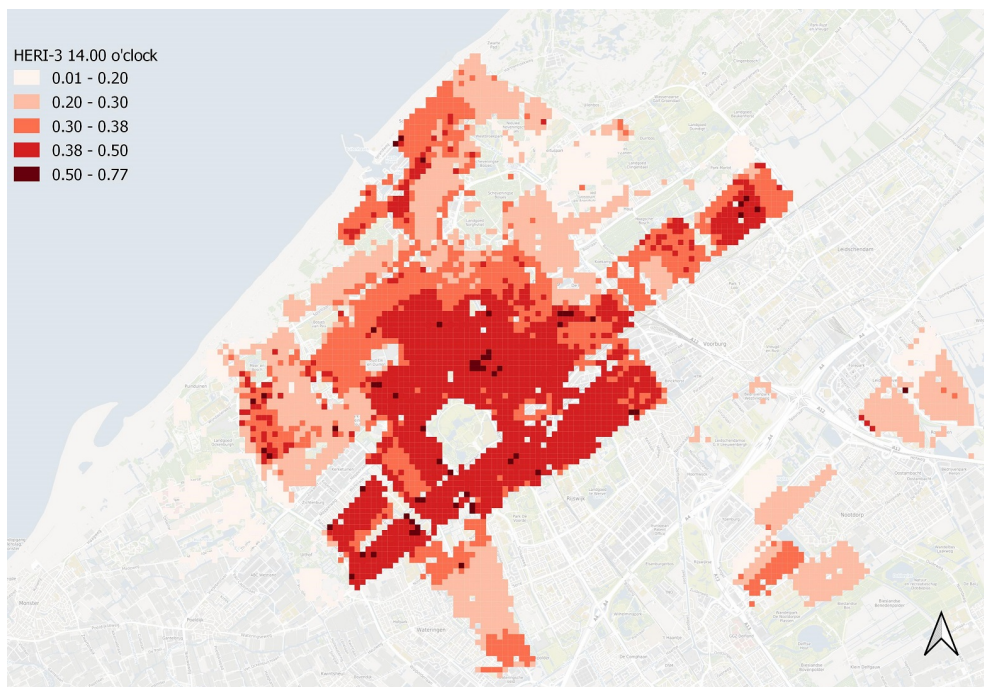


Figure D.5: [HERI-3](#) at 14.00 o'clock in the afternoon at the 27th of July.

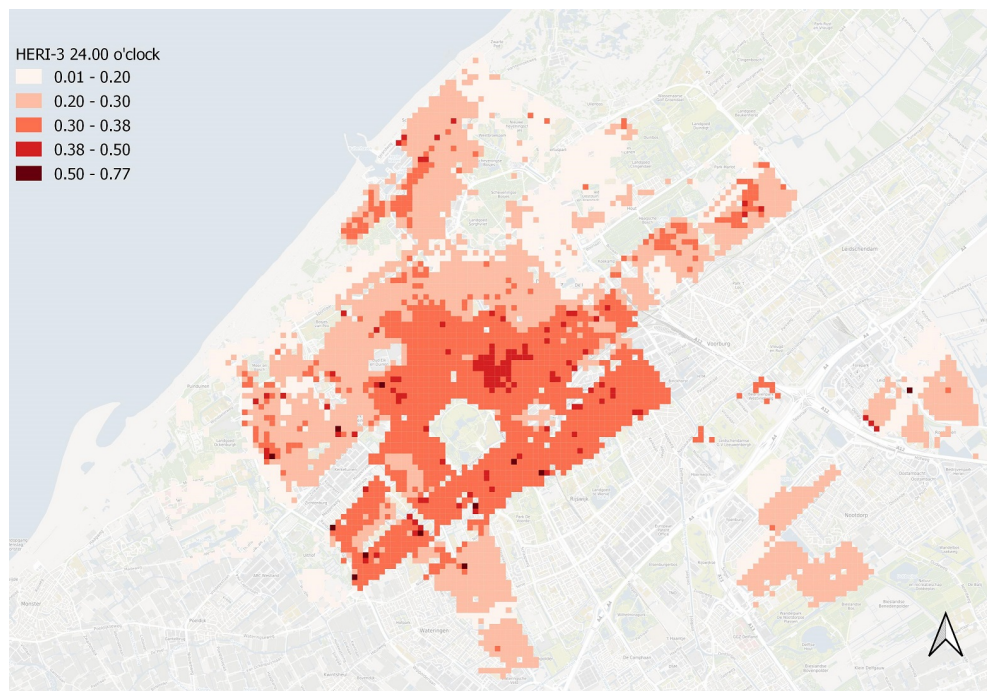


Figure D.6: HERI-3 at 24.00 o'clock at night at the 27th of July.

BIBLIOGRAPHY

- Ali-Toudert, F. (2007). Sustainability and Human Comfort at urban level: Evaluation and Design Guidelines. *Portugal SB 2007 - Sustainable Construction, Materials and Practices: Challenge of the Industry for the New Millennium*, pages 678–685.
- Arup (2014). Reducing urban heat risk. (July).
- Bao, J., Li, X., and Yu, C. (2015). The construction and validation of the heat vulnerability index, a review. *International Journal of Environmental Research and Public Health*, 12(7):7220–7234.
- Basu, R. and Samet, J. M. (2002). Relation between elevated ambient temperature and mortality: A review of the epidemiologic evidence. *Epidemiologic Reviews*, 24(2):190–202.
- Bicol, A., Mikler, V., Breisner, B., and Labrie, M. (2009). Passive design toolkit. *City of Vancouver*, page 114.
- Buscail, C., Upegui, E., and Viel, J. F. (2012). Mapping heatwave health risk at the community level for public health action. *International Journal of Health Geographics*, 11:1–9.
- Centraal Bureau voor de Statistiek (2018). Hitte heeft niet geleid tot veel meer sterfte.
- Chen, Y., Yu, J., Shahbaz, K., and Xevi, E. (2009). A GIS-based sensitivity analysis of multi-criteria weights. (July):3137–3143.
- Cheng, J., Xu, Z., Bambrick, H., Su, H., Tong, S., and Hu, W. (2018). Heatwave and elderly mortality: An evaluation of death burden and health costs considering short-term mortality displacement. *Environment International*, 115(December 2017):334–342.
- Duffy, M. J., Company, T. B., and Sankar, L. (2010). Small wind turbines mounted to existing structures. (August).
- Gago, E. J., Roldan, J., Pacheco-Torres, R., and Ordóñez, J. (2013). The city and urban heat islands: A review of strategies to mitigate adverse effects. *Renewable and Sustainable Energy Reviews*, 25:749–758.
- Gerald, M. and Tebaldi, C. (2004). More Intense , More Frequent , and Longer Lasting Heat Waves in the 21st Century. *Science*, 305(August):994–997.
- Gunawardena, K. R., Wells, M. J., and Kershaw, T. (2017). Utilising green and bluespace to mitigate urban heat island intensity. *Science of the Total Environment*, 584-585:1040–1055.
- Gusmano, M. K. and Rodwin, V. G. (2010). Urban aging, social isolation, and emergency preparedness. *IFA Global Aging*, 6:39–50.
- Gwilliam, J., Fedeski, M., Lindley, S., Theuray, N., and Handley, J. (2006). Methods for assessing risk from climate hazards in urban areas. *Proceedings of the Institution of Civil Engineers - Municipal Engineer*, 159(4):245–255.
- Hien, W. N., Ignatius, M., Eliza, A., Jusuf, S. K., and Samsudin, R. (2012). Comparison of steve and envi-met as temperature prediction models for singapore context. *International Journal of Sustainable Building Technology and Urban Development*, 3(3):197–209.

- Honjo, T. (2009). Thermal Comfort in Outdoor Environment. *Global Environmental Research* ©2009 AIRIES, 13:43–47.
- Hoppe, P. (1999). The physiological equivalent temperature - a universal index for the biometeorological assessment of the thermal environment. *International journal of biometeorology*, 43(2):71–75.
- Huynen, M. M., Martens, P., Schram, D., Weijenberg, M. P., and Kunst, A. E. (2001). The impact of heat waves and cold spells on mortality rates in the Dutch population. *Environmental Health Perspectives*, 109(5):463–470.
- Johansson, E., Thorsson, S., Emmanuel, R., and Krüger, E. (2014). Urban Climate Instruments and methods in outdoor thermal comfort studies – The need for standardization. *Urban Climate*, 10:346–366.
- Johnson, D. P., Stanforth, A., Lulla, V., and Luber, G. (2012). Developing an applied extreme heat vulnerability index utilizing socioeconomic and environmental data. *Applied Geography*, 35(1-2):23–31.
- Johnson, D. P. and Wilson, J. S. (2009). The socio-spatial dynamics of extreme urban heat events: The case of heat-related deaths in Philadelphia. *Applied Geography*, 29(3):419–434.
- Kestens, Y., Brand, A., Fournier, M., Goudreau, S., Kosatsky, T., Maloley, M., and Smargiassi, A. (2011). Modelling the variation of land surface temperature as determinant of risk of heat-related health events. *International Journal of Health Geographics*, 10:1–9.
- Klemm, W., Lenzholzer, S., Heusinkveld, B., and Hove, B. V. (2013). Towards green design guidelines for thermally comfortable streets. pages 10–12.
- KNMI (2019). Hittegolf.
- Lindley, S., Handley, J., McEvoy, D., Peet, E., and Theuray, N. (2013). The Role of Spatial Risk Assessment in the Context of Planning for in UK Urban Areas Adaptation. 33(1):46–69.
- Liu, X. (2013). GIS-Based Local Ordered Weighted Averaging : A Case Study in London , Ontario. (April).
- Lu, J. L. D. (2016). Impact of climate change on human health. *Acta Medica Philippina*, 50(2):91–98.
- Madlener, R. and Sunak, Y. (2011). Impacts of urbanization on urban structures and energy demand: What can we learn for urban energy planning and urbanization management? *Sustainable Cities and Society*, 1(1):45–53.
- Maier, G., Grundstein, A., Jang, W., Li, C., Naeher, L. P., and Shepherd, M. (2013). Assessing the Performance of a Vulnerability Index during Oppressive Heat across Georgia, United States. *Weather, Climate, and Society*, 6(2):253–263.
- Makropoulos, C. K. and Butler, D. (2006). Spatial ordered weighted averaging: Incorporating spatially variable attitude towards risk in spatial multi-criteria decision-making. *Environmental Modelling and Software*, 21(1):69–84.
- Malczewski, J. and Rinner, C. (2015). *Multicriteria Decision Analysis in Geographic Information Science*.
- Maleki, A., Kiesel, K., Vuckovic, M., and Mahdavi, A. (2014). Empirical and computational issues of microclimate simulation. *Lecture Notes in Computer Science (including subseries Lecture Notes in Artificial Intelligence and Lecture Notes in Bioinformatics)*, 8407 LNCS:78–85.

- Matzarakis, A., Muthers, S., and Rutz, F. (2014). Application and comparison of UTCI and pet in temperate climate conditions. *Finisterra*, 49(98):21–31.
- Mayer, H. and Höpfe, P. (1987). Thermal comfort of man in different urban environments. *Theoretical and Applied Climatology*, 38(1):43–49.
- Mayer, H. and Matzarakis, A. (1997). The urban heat island seen from the angle of human-biometeorology. *Proceedings of the International Symposium on Monitoring and Management of the Urban Heat Island*, (May):84–95.
- Mirzaei, P. A. and Haghighat, F. (2010). Approaches to study Urban Heat Island - Abilities and limitations. *Building and Environment*, 45(10):2192–2201.
- Morabito, M., Crisci, A., Gioli, B., Gualtieri, G., Toscano, P., Di Stefano, V., Orlandini, S., and Gensini, G. F. (2015). Urban-hazard risk analysis: Mapping of heat-related risks in the elderly in major Italian cities. *PLoS ONE*, 10(5):1–18.
- Ntarladima, A.-M. (2016). Modelling the Atmospheric Urban Heat Island and its Contributing Spatial Characteristics The case of The Hague, the Netherlands.
- Peel, M. C., Finlayson, B. L., and McMahon, T. A. (2007). Updated world map of the Köppen-Geiger climate classification. *Hydrology and Earth System Sciences*, 11(5):1633–1644.
- Porritt (2012). Assessment of interventions to reduce dwelling overheating during heat waves considering annual energy use and cost.
- Posad, TNO, and Zuid-Holland (2018). Gezond Zuid-Holland 2040. Technical report.
- Reid, C. E., O'Neill, M. S., Gronlund, C. J., Brines, S. J., Brown, D. G., Diez-Roux, A. V., and Schwartz, J. (2009). Mapping community determinants of heat vulnerability. *Environmental Health Perspectives*, 117(11):1730–1736.
- Reid E., C., Mann K., J., Alfasso, R., English B., P., King C., G., Lincoln A., R., Margolis, H. G., Rubado J., D., Sabato E., J., West L., N., Woods, B., Navarro M., K., and Balmes R., J. (2012). Evaluation of a Heat Vulnerability Index on Abnormally Hot Days: An Environmental Public Health Tracking Study. *Environmental Health Perspectives*, 120(5):715–720.
- Rikalovic, A., Cosic, I., and Lazarevic, D. (2014). GIS Based Multi-Criteria Analysis for Industrial Site Selection. *Procedia Engineering*, 69:1054–1063.
- Rosheidat, A., Hoffman, D., and Bryan, H. (2008). Visualizing Pedestrian Comfort Using Envi-Met. *SimBuild 2008*, (July):198–205.
- Saaty, T. L. (2008). Decision making with the analytic hierarchy process. *International Journal of Services Sciences*, 1(1):83.
- Shishegar, N. (2013). Street Design and Urban Microclimate: Analyzing the Effects of Street Geometry and Orientation on Airflow and Solar Access in Urban Canyons. *Journal of Clean Energy Technologies*, 1(1):52–56.
- Siddayao, G. P., Valdez, S. E., and Fernandez, P. L. (2014). Analytic Hierarchy Process (AHP) in Spatial Modeling for Floodplain Risk Assessment. *International Journal of Machine Learning and Computing*, 4(5):450–457.
- Stone, B., Hess, J. J., and Frumkin, H. (2010). Urban form and extreme heat events: Are sprawling cities more vulnerable to climate change than compact cities? *Environmental Health Perspectives*, 118(10):1425–1428.
- Tan, J. (2008). Commentary: People's vulnerability to heat wave. *International Journal of Epidemiology*, 37(2):318–320.

- Tomassini, C., Glaser, K., Wolf, D. A., Broese van Groenou, M. I., and Grundy, E. (2004). Living arrangements among older people: an overview of trends in Europe and the USA. *Population trends*, (115):24–34.
- Tomlinson, C. J., Chapman, L., Thornes, J. E., and Baker, C. J. (2011). Including the urban heat island in spatial heat health risk assessment strategies: a case study for Birmingham, UK. *Australian Library Journal*, 42(10):1–14.
- Uejio, C. K., Wilhelmi, O. V., Golden, J. S., Mills, D. M., Gulino, S. P., and Samenow, J. P. (2011). Intra-urban societal vulnerability to extreme heat: The role of heat exposure and the built environment, socioeconomics, and neighborhood stability. *Health and Place*, 17(2):498–507.
- van der Hoeven, F. and Wandl, A. (2018). *Haagse Hitte*. TU Delft Open.
- Van Hove, L. W. A., Steeneveld, G. J., Jacobs, C. M. J., Heusinkveld, B. G., Elbers, J. A., Moors, E. J., and Holtslag, A. A. M. (2011). Assessment based on a literature review, recent meteorological observations and datasets provided by hobby meteorologists Exploring the Urban Heat Island Intensity of Dutch cities.
- Vandentorren, S., Bretin, P., Zeghnoun, A., Mandereau-Bruno, L., Croisier, A., Cochet, C., Ribéron, J., Siberan, I., Declercq, B., and Ledrans, M. (2006). August 2003 heat wave in France: Risk factors for death of elderly people living at home. *European Journal of Public Health*, 16(6):583–591.
- Vaneckova, P., Beggs, P. J., and Jacobson, C. R. (2010). Spatial analysis of heat-related mortality among the elderly between 1993 and 2004 in Sydney, Australia. *Social Science and Medicine*, 70(2):293–304.
- Vulnerability, H. (2015). Predicting hospitalization for heat-related illness. (6):606–612.
- Waag (2013). All buildings in the Netherlands, shaded by the year of construction.
- Williams, A. A., Spengler, J. D., Catalano, P., Allen, J. G., and Cedeno-Laurent, J. G. (2019). Building Vulnerability in a Changing Climate: Indoor Temperature Exposures and Health Outcomes in Older Adults Living in Public Housing during an Extreme Heat Event in Cambridge, MA. *International Journal of Environmental Research and Public Health*, 16(13):2373.
- Wolf, T. and McGregor, G. (2013). The development of a heat wave vulnerability index for London, United Kingdom. *Weather and Climate Extremes*, 1(August 2003):59–68.

COLOPHON

This document was typeset using L^AT_EX. The document layout was generated using the `arsclassica` package by Lorenzo Pantieri, which is an adaption of the original `classicthesis` package from André Miede.

